Parahydrogen-induced polarization at zero magnetic field

Mark C. Butler, Gwendal Kervern, Thomas Theis, Micah P. Ledbetter, Paul J. Ganssle et al.

Citation: J. Chem. Phys. **138**, 234201 (2013); doi: 10.1063/1.4805062
View online: http://dx.doi.org/10.1063/1.4805062
View Table of Contents: http://jcp.aip.org/resource/1/JCPSA6/v138/i23
Published by the AIP Publishing LLC.

Parahydrogen-induced polarization at zero magnetic field

Mark C. Butler,[1,2,a)] Gwendal Kervern,[1,2,b)] Thomas Theis,[1,2,c)] Micah P. Ledbetter,[3] Paul J. Ganssle,[1,2] John W. Blanchard,[1,2] Dmitry Budker,[3,4] and Alexander Pines[1,2]
[1]*Materials Sciences Division, Lawrence Berkeley National Laboratory, Berkeley, California 94720, USA*
[2]*Department of Chemistry, University of California, Berkeley, California 94720, USA*
[3]*Department of Physics, University of California, Berkeley, California 94720, USA*
[4]*Nuclear Science Division, Lawrence Berkeley National Laboratory, Berkeley, California 94720, USA*

(Received 26 February 2013; accepted 30 April 2013; published online 21 June 2013)

We use symmetry arguments and simple model systems to describe the conversion of the singlet state of parahydrogen into an oscillating sample magnetization at zero magnetic field. During an initial period of free evolution governed by the scalar-coupling Hamiltonian H_J, the singlet state is converted into scalar spin order involving spins throughout the molecule. A short dc pulse along the z axis rotates the transverse spin components of nuclear species I and S through different angles, converting a portion of the scalar order into vector order. The development of vector order can be described analytically by means of single-transition operators, and it is found to be maximal when the transverse components of I are rotated by an angle of $\pm\pi/2$ relative to those of S. A period of free evolution follows the pulse, during which the vector order evolves as a set of oscillating coherences. The imaginary parts of the coherences represent spin order that is not directly detectable, while the real parts can be identified with oscillations in the z component of the molecular spin dipole. The dipole oscillations are due to a periodic exchange between I_z and S_z, which have different gyromagnetic ratios. The frequency components of the resulting spectrum are imaginary, since the pulse cannot directly induce magnetization in the sample; it is only during the evolution under H_J that the vector order present at the end of the pulse evolves into detectable magnetization.
 [http://dx.doi.org/10.1063/1.4805062]

I. INTRODUCTION

The use of parahydrogen to hyperpolarize nuclear-spin samples[1] has proven to be an efficient and versatile technique in nuclear magnetic resonance (NMR). Parahydrogen can be added chemically to a substrate molecule,[2,3] or it can be coupled reversibly to a ligand within a metal complex.[4,5] Spin order originating from parahydrogen has been exploited for a variety of applications, including medical imaging,[6] elucidation of reaction mechanisms,[7] generation of long-lived spin states,[8,9] imaging of catalysis,[10] and quantum computing.[11]

Recent experiments[12,13] have demonstrated that the sensitivity of zero-field NMR spectroscopy can also be enhanced by parahydrogen-induced polarization (PHIP). Zero-field NMR[14–17] shows promise as a tool complementary to conventional high-field NMR, both with regard to information content and instrumentation. For heteronuclear spin systems in liquids, the zero-field spectrum is determined by a network of scalar couplings that extends throughout the molecule and is sensitive to microscopic degrees of freedom. This network is qualitatively different at zero field than at high field, since scalar couplings in zero-field systems are not truncated by the fast precession of spins at different Larmor frequencies. Linewidths in the resulting spectra are narrow,[14–16] due to the elimination of inhomogeneities associated with strong applied fields. The use of an atomic magnetometer for signal detection[18–20] allows for a low-cost, portable[21] spectrometer that does not require cryogens. Samples can be prepolarized by thermal equilibration in an external magnetic field and then shuttled into the zero-field detection region.[14,16] An alternative to thermal prepolarization is to use a hyperpolarization method; in particular, zero-field PHIP yields strong signals without the need for isotope enrichment or sample shuttling.[12,13]

The singlet state of parahydrogen has no dipole moment, and the spherical symmetry of this state must be broken in order to convert the singlet into a detectable magnetization in the sample. A variety of methods have been developed for performing this conversion of spin order under various experimental conditions, and an underlying theme of these methods is the use of a difference in Larmor frequencies to break the spherical symmetry of the initial state. For polarization of H nuclei, chemical-shift differences are typically used to break the symmetry of the singlet,[1–3] while schemes for polarizing heteronuclei exploit frequency differences associated with distinct gyromagnetic ratios.[22]

In zero-field experiments that use PHIP, the spherical symmetry is broken by means of a short dc pulse that causes different nuclear species to precess through different angles. The pulse follows an initial polarization period during which parahydrogen is introduced into the sample. Free evolution

a)Electronic mail: mrkcbutler@gmail.com. Present address: William R. Wiley Environmental Molecular Sciences Laboratory, Pacific Northwest National Laboratory, Richland, Washington 99352, USA.
b)Present address: Méthodologie RMN, Faculté des Sciences et Technologies, Université de Lorraine, 54506 Vandœuvre-lès-Nancy, France.
c)Present address: Department of Chemistry, Duke University, Durham, North Carolina 27708, USA.

under the scalar-coupling Hamiltonian causes spin order to spread through analyte molecules during this period. The spin evolution can begin with a hydrogenation reaction that incorporates parahydrogen into the molecule,[12] or with the reversible binding of parahydrogen and the analyte molecule to the same metal complex (nonhydrogenative PHIP, or NH-PHIP).[13] In the case where the molecule binds to a metal complex, the polarization period is divided into subperiods governed by distinct spin Hamiltonians, since dissociation of the molecule from the complex changes the network of scalar couplings, as well as causing the loss of correlations between the spins of the analyte molecule and the spins remaining in the complex.[5] After the polarization interval, the spin state is an average over different periods of free evolution. Since the initial spin state and the scalar-coupling Hamiltonian H_J are both spherically symmetric, the density matrix corresponding to the averaged spin state is a scalar operator.

When the scalar spin order involves distinct nuclear species I and S, its symmetry can be broken by a dc pulse. The components of I and S transverse to the magnetic field of the pulse precess through different angles, and a portion of the scalar order is converted to vector order, i.e., spin order that transforms as a vector under rotations of the full spin system. After the pulse, the vector order evolves under H_J, yielding an NMR signal.

This paper describes the conversion of the singlet state of parahydrogen into an oscillating sample magnetization in a zero-field environment. The symmetry of the initial state, the scalar-coupling Hamiltonian, and the pulse Hamiltonian impose significant constraints on the evolution; we present a description of zero-field PHIP and NH-PHIP that takes account of these constraints and highlights aspects of the spin physics that can be understood qualitatively. Simple model systems are used for purposes of illustration. The main body of the paper is divided into three sections, which separately discuss the development of spin order during the polarization period, the conversion of the scalar order into vector order by means of the pulse, and the evolution of the vector order during the detection period.

II. DEVELOPMENT OF SCALAR SPIN ORDER

We begin by considering the polarization period, in which a singlet state involving two protons I_1 and I_2 develops into scalar order involving multiple spins in the molecule. For simplicity, we neglect the effects of relaxation, and we assume that I_1 and I_2 are introduced suddenly into an unpolarized network of coupled spins, without perturbation of the singlet.[1,5] The initial density matrix is

$$\rho_0 = \frac{1}{4} - \mathbf{I}_1 \cdot \mathbf{I}_2,$$

where normalization has been neglected. The density matrix representing the system at the end of the polarization period is denoted by ρ_1.

Since the experiments currently of greatest interest involve rare heteronuclei at natural abundance, we assume throughout this paper that the molecule contains protons I_n and a single heteronucleus $S = 1/2$. For an N-spin system, the scalar-coupling Hamiltonian is

$$H_J = \sum_{n=1}^{N-1} 2\pi J_{Sn}\, \mathbf{S} \cdot \mathbf{I}_n + \sum_{m<n} 2\pi J_{mn}\, \mathbf{I}_m \cdot \mathbf{I}_n,$$

where J_{Sn} and J_{mn} are coupling constants that are conventionally expressed in Hz. (Consistent with this convention, energy eigenvalues are expressed in Hz throughout this paper.) The gyromagnetic ratios of the two nuclear species are denoted by γ_I and γ_S. The summed angular momentum of the protons is

$$\mathbf{I} = \sum_{n=1}^{N-1} \mathbf{I}_n, \tag{1}$$

and the total angular momentum is

$$\mathbf{F} = \mathbf{S} + \mathbf{I}.$$

Section II A analyzes the evolution of the three-spin system in the case where parahydrogen is chemically added to a substrate molecule. An analytic expression for the density matrix $\rho(t)$ is derived, and the oscillating spin order is found to include contributions from two-spin scalar products as well as from the scalar triple product. Averaging over the oscillations of $\rho(t)$ gives a formula for ρ_1. The discussion of this section is complementary to previous analyses of formally equivalent systems, which have obtained expressions for ρ_1 without analyzing the time evolution of the spin order.[9,23] In the case where two of the three scalar couplings are truncated due to the presence of a strong magnetic field, a detailed description of the evolution has previously been given,[24] and the discussion in Sec. II A provides a similarly detailed description for a system in which none of the scalar couplings is truncated.

While this approach can in principle be extended to larger systems, our initial investigations showed that the description is significantly more complicated for the four-spin system than for the three-spin system. For larger systems, an alternative approach is needed for qualitative understanding of the spin physics. Sections II B and II C describe the spin order present in the N-spin system at the end of the polarization period, emphasizing simplifications associated with the spherical symmetry of the initial state and the scalar-coupling Hamiltonian H_J. Section II B shows that for zero-field experiments in which parahydrogen is added chemically to a substrate molecule, the development of scalar spin order can be associated with a change of basis: the initial density matrix ρ_0 has a simple structure in a basis obtained by addition of angular momenta, while ρ_1 has a simple structure in a basis of energy eigenstates. Mixing of angular-momentum manifolds for the change of basis is governed by a set of multidimensional rotation matrices R_F, each labeled with a distinct value of the total angular momentum F. The details of the scalar-coupling network affect the spin order represented by ρ_1 only through these rotation matrices. In Sec. II C, we show that for zero-field PHIP and NH-PHIP, ρ_1 can be expressed as a linear combination of simple scalar operators. This expansion of ρ_1 is used in Sec. III to analyze the development of vector order during the pulse.

In order to avoid obscuring the qualitative content of the analysis with abstract arguments, we focus much of the discussion in this paper on the three-spin system. The results

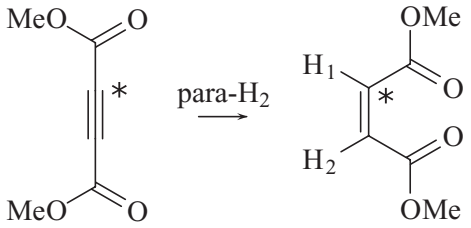

FIG. 1. Addition of parahydrogen to dimethyl acetylenedicarboxylate to form dimethyl maleate. When the reaction product contains a single ^{13}C nucleus in the vinyl group, the hyperpolarized molecule can be modeled as a three-spin system.

obtained by considering the symmetry of this system can be generalized to N spins using arguments outlined in the discussion. For purposes of illustration, we frequently adopt the further simplifying assumption that the coupling between spins S and I_1 is much stronger than the couplings involving I_2:

$$|J_{S1}| \gg |J_{S2}|, |J_{12}|. \tag{2}$$

Relation (2) allows the weak couplings to be treated as a perturbation. In addition to serving as an example, the three-spin system with one strong coupling is interesting because there is a simple physical interpretation of the development of scalar order in the system, discussed in Sec. II B 2.

Figure 1 shows an experimental example of a three-spin system, obtained by adding parahydrogen to dimethyl acetylenedicarboxylate to form dimethyl maleate (DMM). For experiments in which ^{13}C is present at natural abundance, the signal is primarily generated by molecules that have a single ^{13}C nucleus. The isotopomer of DMM with ^{13}C in the vinyl group can be modeled as a three-spin system, since the couplings between the vinyl group and the methyl protons are weak. Consistent with (2), this system has a strong single-bond coupling $J_{S1} \approx 170$ Hz and two weak couplings $|J_{S2}|, |J_{12}| \lesssim 10$ Hz between nuclei separated by more than one bond. The zero-field spectrum of hyperpolarized DMM is presented in Sec. IV.

A. Evolution of the three-spin system

We first consider the coherent evolution of a three-spin system obtained by adding parahydrogen to a substrate molecule, as in Fig. 1. Experimentally, hydrogenation occurs continuously during a polarization period in which parahydrogen is bubbled through the sample in the presence of a homogenous catalyst. With the effects of relaxation neglected, the density matrix ρ_1 that represents the resulting ensemble of polarized molecules is found by taking the time average of $\rho(t)$, the density matrix that describes the coherent evolution of a hydrogenated molecule.

The coherent evolution is governed by the Liouville-von Neumann equation,

$$\frac{d\rho}{dt} = -i\,[H_J, \rho]\,, \tag{3}$$

where

$$H_J = 2\pi\,(J_{S1}\,\mathbf{S}\cdot\mathbf{I}_1 + J_{S2}\,\mathbf{S}\cdot\mathbf{I}_2 + J_{12}\,\mathbf{I}_1\cdot\mathbf{I}_2)\,.$$

We define the operator

$$\Gamma = \mathbf{I}_1 \cdot (\mathbf{I}_2 \times \mathbf{S}). \tag{4}$$

This definition is motivated by the observation that

$$i\Gamma = [\mathbf{I}_1\cdot\mathbf{I}_2, \mathbf{S}\cdot\mathbf{I}_1] = [\mathbf{S}\cdot\mathbf{I}_1, \mathbf{S}\cdot\mathbf{I}_2] = [\mathbf{S}\cdot\mathbf{I}_2, \mathbf{I}_1\cdot\mathbf{I}_2]\,, \tag{5}$$

an identity obtained by means of commutator algebra. Substituting ρ_0 into the right side of Eq. (3) and using Eq. (5) to simplify shows that the derivative $d\rho/dt$ is initially proportional to Γ. Since the commutator of Γ with any scalar-product operator is itself a linear combination of scalar-product operators, the higher-order derivatives of $\rho(t)$ are contained in the space spanned by the operators $\mathbf{I}_1\cdot\mathbf{I}_2$, $\mathbf{S}\cdot\mathbf{I}_1$, $\mathbf{S}\cdot\mathbf{I}_2$, and Γ. During a period of coherent evolution, the density matrix can thus be written as

$$\rho(t) = a(t)\mathbf{I}_1\cdot\mathbf{I}_2 + b(t)\mathbf{S}\cdot\mathbf{I}_1 + c(t)\mathbf{S}\cdot\mathbf{I}_2 + g(t)\Gamma, \tag{6}$$

where the term proportional to the identity has been dropped.

Substitution of Eq. (6) into Eq. (3) and evaluation of the commutators yields

$$\begin{aligned}\frac{d\rho}{dt} = {}& \frac{g(t)}{2}\,(\alpha\mathbf{I}_1\cdot\mathbf{I}_2 + \beta\mathbf{S}\cdot\mathbf{I}_1 + \gamma\mathbf{S}\cdot\mathbf{I}_2)\\ & -[\alpha\,a(t) + \beta\,b(t) + \gamma\,c(t)]\Gamma,\end{aligned} \tag{7}$$

where

$$\begin{aligned}\alpha &= 2\pi\,(J_{S1} - J_{S2})\,,\\ \beta &= 2\pi\,(J_{S2} - J_{12})\,,\\ \gamma &= 2\pi\,(J_{12} - J_{S1})\,.\end{aligned}$$

Since

$$\frac{d\rho}{dt} = \frac{d}{dt}a(t)\,\mathbf{I}_1\cdot\mathbf{I}_2 + \frac{d}{dt}b(t)\,\mathbf{S}\cdot\mathbf{I}_1 + \frac{d}{dt}c(t)\,\mathbf{S}\cdot\mathbf{I}_2 + \frac{d}{dt}g(t)\,\Gamma,$$

it follows that

$$\begin{aligned}\frac{d}{dt}a(t) &= \frac{\alpha}{2}\,g(t),\\ \frac{d}{dt}b(t) &= \frac{\beta}{2}\,g(t),\\ \frac{d}{dt}c(t) &= \frac{\gamma}{2}\,g(t),\\ \frac{d}{dt}g(t) &= -[\alpha\,a(t) + \beta\,b(t) + \gamma\,c(t)].\end{aligned} \tag{8}$$

Differentiation of the last line gives

$$\frac{d^2}{dt^2}g(t) + \frac{\alpha^2+\beta^2+\gamma^2}{2}\,g(t) = 0. \tag{9}$$

From the normalized density matrix for the three-spin system, we obtain $a(0) = -1/2$ and $b(0) = c(0) = g(0) = 0$. The solution to Eq. (9) determined by these initial conditions is

$$g(t) = \frac{\alpha}{2\omega}\sin\omega t, \tag{10}$$

where

$$\omega = \sqrt{\frac{(\alpha^2+\beta^2+\gamma^2)}{2}}.$$

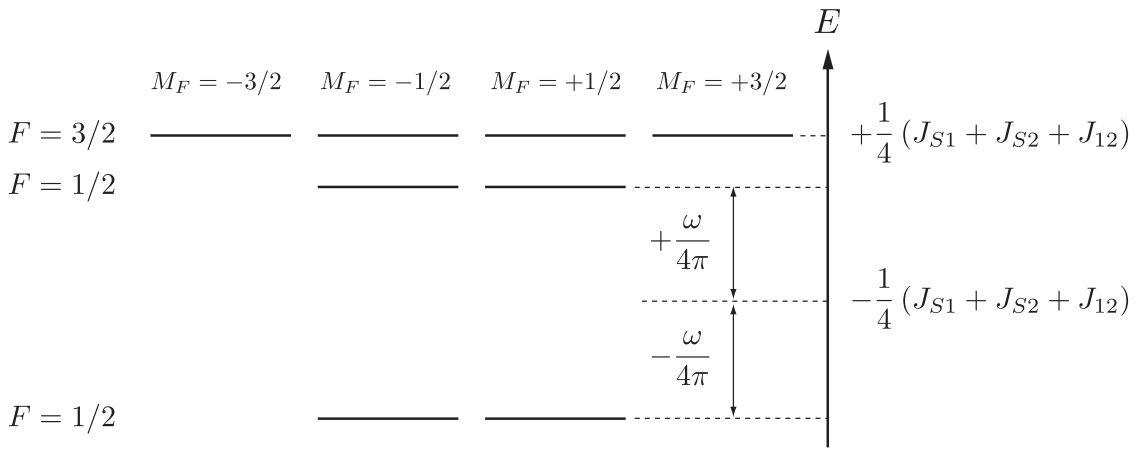

FIG. 2. Energy levels for the three-spin system. Each energy level is an angular-momentum manifold with a well-defined value of F. The degenerate states are labeled with M_F, the z component of total angular momentum. On the right side of the figure, energies are expressed in Hz. Since the initial density matrix has no population in the manifold with $F = 3/2$, the evolution is restricted to the space spanned by the two manifolds with $F = 1/2$. The system therefore oscillates only at frequency $\omega/2\pi$, which corresponds to the energy difference between these two manifolds.

Substitution of Eq. (10) into the first three lines of Eq. (8) and integration of the differential equations gives

$$\begin{aligned} a(t) &= -\frac{1}{2} + \frac{\alpha^2}{4\omega^2}(1 - \cos\omega t), \\ b(t) &= \frac{\alpha\beta}{4\omega^2}(1 - \cos\omega t), \\ c(t) &= \frac{\alpha\gamma}{4\omega^2}(1 - \cos\omega t). \end{aligned} \tag{11}$$

An interesting feature of Eqs. (10) and (11) is that the evolution of $\rho(t)$ simply consists of oscillations at angular frequency ω. To understand this result, we first note that since H_J is invariant with respect to rotations of the full spin system, the energy eigenstates can be grouped into degenerate angular-momentum manifolds. Formally, this property of the eigenstates follows from the fact that H_J commutes with $\mathbf{F}$, the vector operator for the total angular momentum. Figure 2 shows the energy levels of the system, which consist of two manifolds with $F = 1/2$ and one with $F = 3/2$, the values obtained by adding the angular momenta of three spins 1/2. In general, coherences at three different frequencies can contribute to the evolution. However, ρ_0 has no population in the manifold with $F = 3/2$, since the system consists of a heteronucleus $S = 1/2$ and a two-spin singlet with $I = 0$, where I is the proton angular momentum defined by Eq. (1). The initial angular momentum of the system is therefore $F = 1/2$, and since this value is conserved during evolution governed by H_J, coherences involving states of the $F = 3/2$ manifold do not develop. The system can oscillate at only a single frequency, determined by the energy difference between the two $F = 1/2$ manifolds.

Another interesting property of the evolution is that

$$\frac{d}{dt}[a(t) + b(t) + c(t)] = 0,$$

as can be seen from Eq. (8), in combination with the fact that $\alpha + \beta + \gamma = 0$. This restriction on the evolution is due to the form of H_J, rather than the initial state. The sum $(a + b + c)$ is conserved because the operator

$$\mathbf{I}_1 \cdot \mathbf{I}_2 + \mathbf{S} \cdot \mathbf{I}_1 + \mathbf{S} \cdot \mathbf{I}_2 = \frac{1}{2}\left(\mathbf{F}^2 - \mathbf{I}_1^2 - \mathbf{I}_2^2 - \mathbf{S}^2\right)$$

commutes with H_J. A similar conservation law holds for the N-spin system: the sum of the coefficients of all scalar-product operators is constant.

We assume that the polarization period is long compared to the characteristic time for evolution under H_J. Since hydrogenation occurs continuously as parahydrogen is bubbled through the sample, the ensemble of hydrogenated molecules present at the end of the polarization period is represented by the time average of $\rho(t)$. Replacing the coefficients of Eqs. (10) and (11) by their time-averaged components, we obtain

$$\begin{aligned} \rho_1 = \frac{1}{8} + \left(-\frac{1}{2} + \frac{\alpha^2}{4\omega^2}\right)\mathbf{I}_1 \cdot \mathbf{I}_2 \\ + \frac{\alpha\beta}{4\omega^2}\mathbf{S} \cdot \mathbf{I}_1 + \frac{\alpha\gamma}{4\omega^2}\mathbf{S} \cdot \mathbf{I}_2. \end{aligned} \tag{12}$$

Note that ρ_1 does not include a contribution from the operator Γ. Appendix A shows that this is a consequence of the different symmetries of Γ and ρ_1 under time reversal.

In the case where the two protons have the same coupling to the heteronucleus, Eq. (12) reduces to the formula for the normalized initial density matrix ρ_0. The scalar-coupling Hamiltonian commutes with ρ_0 in this case, and so the initial singlet state does not evolve during the polarization period. Since the pulsed magnetic field that follows the polarization period induces a rotation of the proton spin order, the singlet is preserved by the pulse, and there is no signal during the ensuing detection period. This conclusion can be generalized to the N-spin system: there is no signal if heteronuclear scalar order does not develop during the polarization period, since proton scalar order is preserved by the pulse. In particular, there is no signal when all protons have the same coupling to the heteronucleus.

Returning to the general case, we note that an alternative description of the polarized three-spin system can be found by expressing ρ_1 in the eigenbasis of H_J. Straightforward

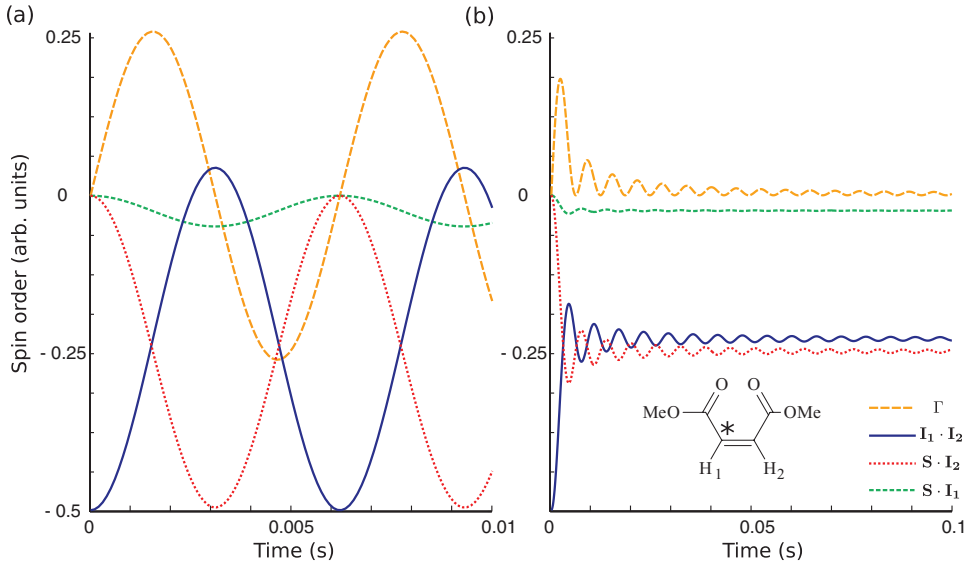

FIG. 3. Simulated evolution of the scalar spin order in the isotopomer of dimethyl maleate that has ^{13}C in the vinyl group. The molecule is modeled as a three-spin system containing protons I_1 and I_2 and a ^{13}C nucleus S. The curves represent the oscillating coefficients in the expansion of the density matrix given by Eq. (6). In the lower-right corner of the figure, each curve is labeled with the corresponding operator from the expansion. (a) Coherent evolution starting from the singlet state at time $t = 0$. (b) Averaging of the spin order during a polarization period in which hydrogenation occurs continuously as parahydrogen is bubbled through the sample. The coupling constants used in the simulations were $J_{S1} = 167.2$ Hz, $J_{S2} = -2.2$ Hz, and $J_{12} = 13.0$ Hz, consistent with the simulation of the experimental zero-field spectrum shown in Fig. 5.

algebraic manipulations show that ρ_1 is diagonal in this basis, and the population of a state with angular momentum $F = 1/2$ and energy

$$E_n = -\frac{1}{4}(J_{S1} + J_{S2} + J_{12}) \pm \frac{\omega}{4\pi} \tag{13}$$

is

$$\rho_{nn} = \frac{1}{4} \mp \frac{\pi(-J_{S1} - J_{S2} + 2J_{12})}{4\omega}. \tag{14}$$

The development of scalar spin order in a three-spin system is illustrated in Fig. 3, which shows how the isotopomer of dimethyl maleate with ^{13}C in the vinyl group evolves during the polarization period. Oscillations in the spin order are quickly averaged to a negligible level, and the initial spin order $(-1/2)\mathbf{I}_1 \cdot \mathbf{I}_2$ evolves into the sum of scalar products given by Eq. (12). Although $\rho(t)$ includes a significant contribution from Γ during the coherent evolution, as shown in Fig. 3(a), this contribution does not survive the averaging process shown in Fig. 3(b). From Eq. (8), the coherent evolution can be interpreted as an interconversion of Γ and the scalar-product terms, roughly analogous to the exchange between potential and kinetic energy in a harmonic oscillator. A maximal coefficient for Γ corresponds to fast change in the coefficients of the scalar products, which evolve to their extrema as the coefficient of Γ reaches zero. Formally, Γ oscillates $\pm 90^\circ$ out of phase with the scalar-product terms.

B. Structure of the scalar order

For experiments in which larger systems are polarized by means of PHIP or NH-PHIP, the structure of the spin order present at the end of the polarization period can be characterized by taking account of the constraints imposed by the symmetry of the initial state and the Hamiltonian. Section II B 1 discusses the structure of the spin order in a three-spin system obtained by adding parahydrogen to a substrate molecule. We define basis sets B_1 and B_2, which, respectively, yield simple forms for the initial density matrix ρ_0 and for ρ_1, the density matrix representing the system at the end of the polarization period. The constraints imposed by symmetry can be highlighted by considering the transformation of ρ_0 from basis B_1 to B_2. Section II B 2 presents an example calculation for the three-spin system with $|J_{S1}| \gg |J_{S2}|, |J_{12}|$ and discusses a physical interpretation of the spreading of scalar order in this system.

1. Unpolarized manifolds

Expressing ρ_0 and ρ_1 in appropriate basis sets shows how the structure of the spin order changes during the polarization period. For a three-spin system obtained by adding parahydrogen to a substrate molecule, we use the Clebsch-Gordan coefficients to calculate a basis set of states $|F, M_F, I\rangle$, where M_F is the z component of the total angular momentum, and I is the summed angular momentum of the two protons. Addition of I_1 and I_2 yields singlet and triplet manifolds of I, and addition of S to these manifolds yields the states $|F, M_F, I\rangle$. The resulting basis set, which we denote by B_1, divides the state space into the three manifolds listed on the left side of Table I. The population of the initial singlet state is entirely contained in the manifold with quantum numbers $(F = 1/2, I = 0)$; indeed, the only nonzero elements of ρ_0 in this basis set are the equal populations of the two states $|1/2, \pm 1/2, 0\rangle$.

We noted in Sec. II A that the energy eigenstates of the three-spin system can be grouped into degenerate

TABLE I. Structure of the scalar order in a three-spin system obtained by adding parahydrogen to a substrate molecule. The initial density matrix ρ_0 is diagonalized by a basis of states $|F, M_F, I\rangle$, where I is the summed angular momentum of the two protons. These states can be grouped into the manifolds listed on the left side of the table. The manifold with $F = 3/2$ is a degenerate energy level with spin energy $E_1 = (J_{S1} + J_{S2} + J_{12})/4$. At the end of the polarization period, the density matrix ρ_1 is diagonalized by a basis of energy eigenstates $|F, M_F, E\rangle$. The corresponding manifolds are listed on the right side of the table. The energies E_2 and E_3 and the population a, which can be evaluated using Eqs. (13) and (14), depend on the details of the scalar-coupling network.

Structure of the initial scalar order		Structure of the final scalar order	
Manifold	Population	Manifold	Population
$F = 3/2, I = 1, E_1$	0	$F = 3/2, I = 1, E_1$	0
$F = 1/2, I = 1$	0	$F = 1/2, E_2$	a
$F = 1/2, I = 0$	1	$F = 1/2, E_3$	$1-a$

angular-momentum manifolds. The system includes a unique manifold with $F = 3/2$, which is necessarily a degenerate energy level. However, the manifolds with quantum numbers $(F = 1/2, I = 1)$ and $(F = 1/2, I = 0)$ do not in general consist of energy eigenstates. For a given value of M_F, the Hamiltonian H_J "selects" linear combinations of the two states

$$\begin{aligned} |u\rangle &= |F = 1/2, M_F, I = 1\rangle, \\ |v\rangle &= |F = 1/2, M_F, I = 0\rangle \end{aligned} \tag{15}$$

as eigenstates $|F = 1/2, M_F, E\rangle$, where E is the spin energy. Since H_J is a scalar operator, the Wigner-Eckart theorem implies that the coefficients used for these linear combinations are independent of the value of M_F. The 2×2 matrix R obtained by diagonalizing H_J with respect to a pair of states $|u\rangle$, $|v\rangle$ can thus be considered to govern the mixing of the manifolds $(F = 1/2, I)$ to form manifolds $(F = 1/2, E)$. Appendix A shows that the energy eigenstates can be chosen such that R is an orthogonal matrix, formally associated with a rotation of the Euclidean plane. We let B_2 denote the basis of eigenstates chosen in this way.

The density matrix ρ_1 of the polarized system can be found by transforming ρ_0 from basis B_1 to basis B_2 and then eliminating off-diagonal matrix elements between states of different energy, which correspond to oscillating coherences that do not survive averaging over the distribution of evolution times. As noted in Sec. II A, the coherences present in the three-spin system are between eigenstates with $F = 1/2$. The rotation R determines the initial values of these coherences as well as the eigenstate populations that characterize the polarized system. Formally, the details of the coupling network affect the spin order represented by ρ_1 only through R.

Since the initial density matrix and the Hamiltonian H_J are both scalar operators, ρ_1 is also a scalar operator, and it follows from the Wigner-Eckart theorem that ρ_1 is proportional to the identity within each angular-momentum manifold formed from the energy eigenstates of basis B_2. At the end of the polarization period, the density matrix is specified by the populations of these manifolds, as illustrated by the right side of Table I. Physically, the system is unpolarized within these manifolds, because of the lack of any preferred spatial direction. As we show in Appendix B, this result can be generalized to an N-spin system polarized by hydrogenative PHIP or by NH-PHIP: ρ_1 can be diagonalized by an energy eigenbasis B_2 that divides the state space into degenerate manifolds of F, with ρ_1 proportional to the identity within each manifold. For each of the possible values of F, the manifolds formed by the states of basis B_2 are related through a multidimensional rotation R_F to manifolds obtained by addition of angular momenta. Formally, the scalar spin order that develops in a system polarized by hydrogenative PHIP is determined solely by the rotations R_F, since the net effect of the evolution during the polarization period is to average to zero the initial coherences between states of different energy.

TABLE II. Approximate energy levels of the three-spin system that has $|J_{S1}| \gg |J_{S2}|, |J_{12}|$. The zero-order eigenstates can be written in the form $|F, M_F, F_1\rangle$, where the angular momentum F_1 is the sum of S and I_1. These eigenstates are grouped into the degenerate angular-momentum manifolds listed on the left side of the table. The energies are given to first order in the weak couplings.

Manifold	Spin energy
$F = 3/2, F_1 = 1$	$E_1 = J_{S1}/4 + (J_{S2} + J_{12})/4$
$F = 1/2, F_1 = 1$	$E_2 = J_{S1}/4 - (J_{S2} + J_{12})/2$
$F = 1/2, F_1 = 0$	$E_3 = -3J_{S1}/4$

2. Three-spin system with one strong coupling

We illustrate the conclusions of Sec. II B 1 with calculations for the three-spin system that has $|J_{S1}| \gg |J_{S2}|, |J_{12}|$. The zero-order energy eigenstates and first-order energies are found by diagonalizing the perturbation

$$H_1 = 2\pi\,(J_{S2}\,\mathbf{S}\cdot\mathbf{I}_2 + J_{12}\,\mathbf{I}_1\cdot\mathbf{I}_2) \tag{16}$$

within each degenerate energy level of

$$H_0 = 2\pi\,J_{S1}\,\mathbf{S}\cdot\mathbf{I}_1.$$

The eigenstates of H_0 can be grouped into degenerate manifolds labeled with quantum numbers (F, F_1), where

$$\mathbf{F}_1 = \mathbf{S} + \mathbf{I}_1.$$

These manifolds are obtained by first adding angular momenta S and I_1 to form singlet and triplet manifolds of F_1, and then adding angular momentum I_2, which yields states $|F, M_F, F_1\rangle$. The states are grouped into the angular-momentum manifolds listed in Table II.

With H_1 treated as a weak perturbation, couplings between states that have distinct values of F_1 are neglected, because states derived from the singlet and triplet manifolds of F_1 have different energies under H_0. In particular, state $|F, M_F, F_1\rangle$ would have energy[16]

$$\frac{J_{S1}}{2}[F_1\,(F_1+1) - S\,(S+1) - I_1\,(I_1+1)]$$

in the absence of the perturbation. Since H_1 is a scalar operator, the Wigner-Eckart theorem implies that it cannot couple

states with different values of F. The two manifolds in Table II that have the same value of F have different values of F_1, and it follows that each manifold (F, F_1) is a zero-order energy level of $H_0 + H_1$.[15]

Following the discussion given in Sec. II B 1, we define basis sets B_1 and B_2, where B_1 consists of states $|F, M_F, I\rangle$ and B_2 consists of energy eigenstates $|F, M_F, F_1\rangle$. Note that these two basis sets are both obtained by adding the angular momenta of the three spins: for B_1, the heteronucleus is added last, while for B_2, the weakly coupled spin is added last. The states of B_1 are ordered first by decreasing values of M_F, second by decreasing values of F, and third by decreasing values of I:

$$\begin{aligned} B_1 = \{&|3/2, 3/2, 1\rangle, \\ &|3/2, 1/2, 1\rangle, |1/2, 1/2, 1\rangle, |1/2, 1/2, 0\rangle, \\ &|3/2, -1/2, 1\rangle, |1/2, -1/2, 1\rangle, |1/2, -1/2, 0\rangle, \\ &|3/2, -3/2, 1\rangle\}. \end{aligned} \tag{17}$$

In Eq. (17), states listed on the same line have the same value of M_F. The states of B_2 are similarly ordered, but with F_1 replacing I in the ordering. The 8×8 block-diagonal matrix that converts coordinates in B_1 to coordinates in B_2 is

$$T = \begin{bmatrix} 1 & & & & & & & \\ & 1 & & & & & & \\ & & R & & & & & \\ & & & 1 & & & & \\ & & & & R & & & \\ & & & & & 1 & & \\ & & & & & & & \end{bmatrix},$$

where

$$R = \begin{bmatrix} -1/2 & \sqrt{3}/2 \\ -\sqrt{3}/2 & -1/2 \end{bmatrix}.$$

Since basis sets B_1 and B_2 were both obtained by addition of angular momenta with the Clebsch-Gordan coefficients, the change-of-basis matrix T does not depend on the scalar couplings. Note that R is formally associated with a rotation of the Euclidean plane.

During all stages of the experiment, the 8×8 density matrix is block diagonal when expressed in basis B_1 or B_2. In either basis, it has the form

$$\rho = \begin{bmatrix} 0 & & & \\ & \rho^{(+1/2)} & & \\ & & \rho^{(-1/2)} & \\ & & & 0 \end{bmatrix}, \tag{18}$$

where the 3×3 submatrices $\rho^{(+1/2)}$ and $\rho^{(-1/2)}$ represent the restriction of ρ to the eigenspaces of F_z with eigenvalues $M_F = +1/2$ and $M_F = -1/2$, respectively. In basis B_1, the normalized initial density matrix ρ_0 has

$$\rho_0^{(+1/2)} = \rho_0^{(-1/2)} = \frac{1}{2}\begin{bmatrix} 0 & 0 & 0 \\ 0 & 0 & 0 \\ 0 & 0 & 1 \end{bmatrix}. \tag{19}$$

On the right side of Eq. (19), the elements along the diagonal are populations associated with the manifolds that have quantum numbers

$$\begin{aligned} &(F = 3/2, I = 1), \\ &(F = 1/2, I = 1), \\ &(F = 1/2, I = 0), \end{aligned}$$

where the ordering is from upper left to lower right. Transformation to the energy eigenbasis B_2 gives

$$\rho_0^{(+1/2)} = \rho_0^{(-1/2)} = \frac{1}{2}\begin{bmatrix} 0 & 0 & 0 \\ 0 & 3/4 & -\sqrt{3}/4 \\ 0 & -\sqrt{3}/4 & 1/4 \end{bmatrix}, \tag{20}$$

and elimination of the coherences during the polarization period yields

$$\rho_1^{(+1/2)} = \rho_1^{(-1/2)} = \frac{1}{2}\begin{bmatrix} 0 & 0 & 0 \\ 0 & 3/4 & 0 \\ 0 & 0 & 1/4 \end{bmatrix}. \tag{21}$$

From Eq. (21), the manifold $(F = 1/2, F_1 = 1)$ has 3/4 of the population, while the manifold $(F = 1/2, F_1 = 0)$ has 1/4 of the population. This distribution of population can be rationalized by noting that for a two-spin system containing only I_1 and S, the number of independent states with $F_1 = 1$ is three times the number of independent states with $F_1 = 0$. Immediately after the hydrogenation, I_1 and I_2 are in a singlet state and S is completely unpolarized; in the absence of any information about the relative orientation of I_1 and S, we might guess that the summed population of the states with $F_1 = 1$ would be three times the summed population of the states with $F_1 = 0$. It can be shown that this guess is correct when I_1 and I_2 are described by an arbitrary two-spin state function, with S completely unpolarized. When the protons are initially in a singlet state, the total angular momentum is $F = 1/2$, which imposes the additional constraint that the population of the manifold $(F = 3/2, F_1 = 1)$ is zero. The population of the manifold $(F = 1/2, F_1 = 1)$ is therefore three times that of the manifold $(F = 1/2, F_1 = 0)$.

The modification of the density matrix due to the spreading of spin order can be visualized geometrically. For a given value of M_F, the two states $|u\rangle$, $|v\rangle$ of Eq. (15) are identified with unit vectors in a Euclidean plane whose axes are labeled with u and v. The initial singlet state is oriented along the v axis. Transformation to the eigenstate basis corresponds to a rotation of the two axes; after the rotation, the vector identified with the singlet state has projections $\sqrt{3}/2$ and $-1/2$ along the two axes, and the populations 3/4 and 1/4 are found by squaring these two projections.

As noted in Sec. II B 1, the details of the coupling network affect ρ_1 only through the rotation R. In particular, if we drop the assumption that $|J_{S1}| \gg |J_{S2}|, |J_{12}|$, then the simple numerical values obtained for the matrix elements in Eqs. (20) and (21) are replaced by formulas that depend on the details of the coupling network, but the form of the matrices is unchanged. The system with one strong coupling is a convenient model system because the zero-order eigenstates do not depend on the details of the coupling network, and the transformation between B_1 and B_2 involves simple numerical factors.

The development of scalar order in this system has a natural physical interpretation. In order to motivate this interpretation, we write the density matrix of the polarized system in the form

$$\rho_1 = \frac{1}{2}\left(\frac{1}{4} - \frac{1}{2}\mathbf{F}_1 \cdot \mathbf{I}_2\right). \tag{22}$$

Equation (22) can be compared to a similar expression for the normalized initial density matrix:

$$\rho_0 = \frac{1}{2}\left(\frac{1}{4} - \mathbf{I}_1 \cdot \mathbf{I}_2\right). \tag{23}$$

To understand how the polarization process converts $\mathbf{I}_1 \cdot \mathbf{I}_2$ to $(1/2)\mathbf{F}_1 \cdot \mathbf{I}_2$, we first consider the limiting case where $H_1 = 0$. As in the vector model of the atom,[25,26] the evolution under H_0 can be visualized as precession of $\mathbf{S}$ and $\mathbf{I}_1$ about $\mathbf{F}_1$, which is motionless. Averaging over the precession during the polarization period corresponds to projecting $\mathbf{I}_1$ onto $\mathbf{F}_1$. We denote the resulting projection by $\mathbf{I}_1^{\|}$. Formally, $\mathbf{I}_1^{\|}$ is defined in the singlet and triplet manifolds of F_1, and the projection theorem[27] shows that

$$\mathbf{I}_1^{\|} = \frac{1}{2}\mathbf{F}_1 \tag{24}$$

in each manifold. Equation (24), which is derived for the two-spin system containing S and I_1, can also be considered to define $\mathbf{I}_1^{\|}$ on the state space of the three-spin system. It follows from Eqs. (22) and (24) that

$$\rho_1 = \frac{1}{2}\left(\frac{1}{4} - \mathbf{I}_1^{\|} \cdot \mathbf{I}_2\right). \tag{25}$$

Comparison of Eqs. (23) and (25) shows that averaging over the distribution of evolution times simply causes $\mathbf{I}_1$ to be replaced by its average over the fast precession governed by H_0.

In order to explain why ρ_1 has the same form when the perturbation H_1 is nonzero, we note that the first-order approximation to H_1 can be expressed in the form[15]

$$\begin{aligned} &2\pi\left(J_{S2}\,\mathbf{S}^{\|} \cdot \mathbf{I}_2 + J_{12}\,\mathbf{I}_1^{\|} \cdot \mathbf{I}_2\right) \\ &\quad = 2\pi\left(\frac{J_{S2} + J_{12}}{2}\right)\mathbf{F}_1 \cdot \mathbf{I}_2, \end{aligned} \tag{26}$$

where

$$\mathbf{S}^{\|} = \frac{1}{2}\mathbf{F}_1$$

is the projection of $\mathbf{S}$ onto $\mathbf{F}_1$. We can interpret Eq. (26) to mean that the weakly coupled spin does not "see" the instantaneous states of the strongly coupled spins. To first order, $\mathbf{I}_2$ is coupled instead to $\mathbf{S}^{\|}$ and $\mathbf{I}_1^{\|}$, the averages of $\mathbf{S}$ and $\mathbf{I}_1$ over the fast evolution governed by H_0. Truncation of the weak scalar couplings by the strong scalar coupling therefore gives an effective interaction of the form $\mathbf{F}_1 \cdot \mathbf{I}_2$.[15] During the polarization period, averaging over the evolution governed by H_0 quickly converts the initial singlet order $\mathbf{I}_1 \cdot \mathbf{I}_2$ to $(1/2)\,\mathbf{F}_1 \cdot \mathbf{I}_2$, which does not evolve under H_1, since it commutes with the truncated scalar couplings.

The results obtained from perturbation theory can be compared with the numerical simulation presented in Fig. 3(b), which corresponds to a system where H_0 is larger than H_1 by roughly an order of magnitude. The average over evolution times yields spin order that has nearly equal contributions from $\mathbf{I}_1 \cdot \mathbf{I}_2$ and $\mathbf{S} \cdot \mathbf{I}_2$ and can thus be approximated as having the form $\mathbf{F}_1 \cdot \mathbf{I}_2$. Because the first-order description is not exact for this system, the simulation also shows a contribution from the term $\mathbf{S} \cdot \mathbf{I}_1$, which does not appear in Eq. (22).

C. Complexity of the scalar order

In this section, we characterize the complexity of the scalar order by counting the parameters needed to specify ρ_1 in basis sets B_1 and B_2. In Sec. II B, these basis sets are defined for a three-spin system obtained by adding parahydrogen to a substrate molecule. Appendix B generalizes the definitions to an N-spin system polarized by PHIP or NH-PHIP. Basis B_1 is formed by addition of angular momenta, with the heteronucleus added last, while B_2 is an energy eigenbasis that diagonalizes ρ_1 and divides the state space into degenerate angular-momentum manifolds. We show in this section that ρ_1 can be expressed as a linear combination of scalar operators that have a simple form in basis B_1. The resulting expansion of ρ_1 is used in Sec. III to analyze the development of vector order during the pulse.

For a three-spin system polarized by hydrogenative PHIP, ρ_1 can by specified in the energy eigenbasis B_2 by a single parameter, as shown on the right side of Table I. A single parameter is sufficient because the population of the manifold with $F = 3/2$ is zero, and because the populations of the two manifolds with $F = 1/2$ sum to 1. For a three-spin system polarized by NH-PHIP, two parameters are needed to specify ρ_1 in basis B_2, since the constraint on the population of the manifold with $F = 3/2$ is absent.

A system of N spins 1/2 contains

$$q(N, F) = \frac{N!\,(1 + 2F)}{(N/2 - F)!\,(N/2 + F + 1)!} \tag{27}$$

manifolds of total angular momentum F.[28] For an N-spin system polarized by PHIP or NH-PHIP, the sum

$$Q = \sum_{F=(N \bmod 2)/2}^{N/2} q(N, F)$$

gives a simple estimate of the number of parameters needed to specify ρ_1 in basis B_2. This estimate neglects certain constraints on the density matrix, such as the requirement that the populations sum to 1, but these constraints do not dramatically simplify the formal structure of ρ_1 in systems containing several spins or more. As examples to characterize complexity, we note that a five-spin system has $Q = 10$ while a ten-spin system has $Q = 252$.

An alternative to using the energy eigenbasis to characterize the complexity of the density matrix is to expand ρ_1 as a linear combination of predetermined scalar operators whose definition does not depend on the Hamiltonian. An example of such an expansion is given by Eq. (12), which uses a linear combination of scalar-product operators to describe the scalar order of the three-spin system polarized by hydrogenative PHIP. In generalizing to larger spin systems polarized by PHIP or NH-PHIP, we use the constraints imposed by

symmetry to enumerate a set of orthogonal operators that can make a nonzero contribution to ρ_1. As shown in Appendix A and Appendix B, respectively, ρ_1 is invariant under time reversal as well as under rotations of the full spin system. An expansion of ρ_1 can be obtained by taking account of the constraints associated with invariance under these transformations.

For purposes of illustration, we first consider a three-spin system polarized by NH-PHIP. The Wigner-Eckart theorem implies that a Hermitian scalar operator A expressed in the basis B_1 of Eq. (17) is block diagonal and has the form

$$A = \begin{bmatrix} a_1 & & & \\ & A^{(+1/2)} & & \\ & & A^{(-1/2)} & \\ & & & a_1 \end{bmatrix}, \tag{28}$$

where

$$A^{(+1/2)} = A^{(-1/2)} = \begin{bmatrix} a_1 & 0 & 0 \\ 0 & a_2 & a_4 + ia_5 \\ 0 & a_4 - ia_5 & a_3 \end{bmatrix}, \tag{29}$$

and where the coefficients a_n are real. As in Eq. (18), the superscripts $(+1/2)$ and $(-1/2)$ denote the restriction of the operator to the eigenspaces of F_z with eigenvalues $M_F = +1/2$ and $M_F = -1/2$, respectively. Each of the diagonal elements a_1, a_2, and a_3 is associated with the states $|F, M_F\rangle$ of a single manifold, while the off-diagonal matrix elements $a_4 \pm ia_5$ are between states that have the same values of F and M_F but belong to different manifolds. Equations (28) and (29) implicitly express A as a linear combination of scalar operators, each obtained by setting a single coefficient a_n to 1, with the remaining matrix elements set to zero.

Appendix A shows that since ρ_1 is invariant under rotations and time reversal, its matrix elements are real in a basis obtained by addition of angular momenta with the Clebsch-Gordan coefficients. In particular, the matrix elements of ρ_1 are real when it is expressed in basis B_1. Identifying the operator A in Eqs. (28) and (29) with ρ_1, we conclude that the coefficient a_5 is zero. Four nonzero coefficients appear in the expansion of ρ_1 implicitly given by these equations.

In generalizing these arguments to the N-spin system, we use an arbitrary quantum number X to distinguish the angular-momentum manifolds formed by the states of basis B_1. We divide the state space into subspaces V_F, each spanned by the set of states $|F, M_F, X\rangle$ that are labeled with a particular value of F. Equivalently, V_F can be defined as the eigenspace of $\mathbf{F}^2$ with eigenvalue $F(F+1)$. Since ρ_1 is a scalar operator, it has nonzero matrix elements only between states labeled with the same value of F. It therefore suffices to specify the restriction of ρ_1 to each of the subspaces V_F. We consider an arbitrary V_F, and for each manifold X_n contained in it, we define the operator A_n to be zero outside of the manifold and equal to the identity within it. For each pair of distinct manifolds X_j, X_k belonging to V_F, we define the operator A'_{jk} to have nonzero matrix elements

$$\begin{aligned} &\langle F, M_F, X_j|A'_{jk}|F, M_F, X_k\rangle \\ &\quad = \langle F, M_F, X_k|A'_{jk}|F, M_F, X_j\rangle = 1, \end{aligned} \tag{30}$$

where M_F ranges from $-F$ to $+F$. All matrix elements of A'_{jk} other than those specified by Eq. (30) are zero. Note that the operators A_n are a generalization of the operators obtained by setting a_1, a_2, or a_3 to 1 in the three-spin example, with the remaining coefficients set to zero. The operators A'_{jk} are a generalization of the three-spin operator that has a single nonzero coefficient $a_4 = 1$.

Since ρ_1 is invariant under rotations and time reversal, its matrix elements in basis B_1 are real. The Wigner-Eckart theorem therefore implies that the restriction of ρ_1 to V_F is a linear combination of the orthogonal scalar operators A_n and A'_{jk}. The number of coefficients needed for this linear combination is

$$p(N, F) = q(N, F) + \binom{q(N, F)}{2},$$

where $q(N, F)$ is given by Eq. (27). The full expansion for ρ_1 is obtained by adding together the linear combinations corresponding to the subspaces V_F. The number of coefficients appearing in the full expansion is

$$P = \sum_{F=(N \bmod 2)/2}^{N/2} p(N, F).$$

By way of illustration, we return to the three-spin system polarized by NH-PHIP. For this system, F can take the values 1/2 and 3/2. Since $p(3, 1/2) = 3$ and $p(3, 3/2) = 1$, a total of $P = 4$ coefficients appear in the expansion of ρ_1, as we found above. The expansion has $P = 26$ and $P = 8524$ coefficients for a five-spin system and a ten-spin system, respectively.

III. CONVERSION TO VECTOR ORDER

In describing the conversion of the scalar order to vector order by means of a dc pulse, we begin by considering a two-spin system. The coherent evolution of this system involves only two of the energy eigenstates, and so the system can be modeled as a fictitious spin 1/2 or pseudospin. We let $\tilde{x}$, $\tilde{y}$, $\tilde{z}$ denote the axes of the pseudospin. The scalar order present just before the pulse corresponds to polarization of the pseudospin along the $\tilde{z}$ axis, and the pulse induces a $\pi/2$ flip to $-\tilde{y}$, which represents undetectable vector order. The pseudospin precesses in its transverse plane during the detection period, and its $\tilde{x}$ component represents a signal in the form of oscillating magnetization. This model of the two-spin system is presented in Sec III A, and the model is generalized in Sec. III B to describe the evolution of the N-spin system during the pulse. The state space is decomposed into one-dimensional and two-dimensional subspaces that are not coupled by the pulse. In each two-dimensional space, a pseudospin precesses about an effective field in the $\tilde{x}\tilde{z}$ plane, with all pseudospins precessing at the same frequency, determined by the strength of the dc field and the difference between the gyromagnetic ratios γ_I and γ_S. Optimal conversion of scalar order to vector order corresponds to a $\pm\pi/2$ rotation of the pseudospins, which yields a maximal component along $\pm\tilde{y}$ for pseudospins polarized along $\pm\tilde{z}$ before the pulse. Physically, the conversion is performed by rotating the transverse spin components

of the protons through an angle of $\pm\pi/2$ with respect to the transverse components of the heteronucleus, where the transverse plane is defined by choosing the laboratory-frame z axis to be colinear with the pulsed field.

The pseudospin model exploits the fact that the pulsed field induces a uniform rotation of all protons, and qualitative analysis of the N-spin system using this model requires a basis set of states with a well-defined value of the proton angular momentum I. We develop the pseudospin model using the basis set B_1, which is obtained by addition of angular momenta, with the heteronucleus added last.

For the hydrogenation experiment, the development of scalar spin order during the polarization period is associated with a change from basis B_1 to the energy eigenbasis B_2, followed by the elimination of off-diagonal terms; qualitative analysis of the pulse is facilitated by transforming the resulting density matrix ρ_1 back to basis B_1. As illustrated by calculations presented in Sec. III B, the density matrix that represents the spin system at the end of the pulse, denoted by ρ_2, must then be transformed to the energy eigenbasis for the analysis of the spectrum. The change of basis between B_1 and B_2, characterized by multidimensional rotations R_F that mix angular-momentum manifolds, therefore plays a central role in determining the phases and amplitudes of the peaks in the zero-field spectrum.

A. Two-spin system

Single-transition operators[29] have been used for the analysis of high-field PHIP experiments,[24,30] and they can also be used to describe the conversion of scalar order to vector order in zero-field experiments. Single-transition operators are defined by treating a pair of energy eigenstates involved in a transition as a virtual two-state system.[29] For the two-spin system governed by the Hamiltonian $H_J = 2\pi J_{SI}\,\mathbf{S}\cdot\mathbf{I}$, the states $|F, M_F\rangle$ are energy eigenstates. The single-transition operators for the pair of states $|1, 0\rangle$ and $|0, 0\rangle$ are zero-quantum operators that can be expressed in the form

$$\begin{aligned} \mathcal{Z}_x &= \frac{1}{2}(I_z - S_z), \\ \mathcal{Z}_y &= S_y I_x - S_x I_y, \\ \mathcal{Z}_z &= S_x I_x + S_y I_y. \end{aligned} \tag{31}$$

The term "zero-quantum" is inherited from high-field NMR, where the dominant term in the spin Hamiltonian is the interaction with the static field applied along the z axis. In the context of high-field NMR, a zero-quantum transition involves two states having the same z component of total angular momentum.

The operators defined by Eq. (31) satisfy the commutation relations for angular momentum. As we show below, a simple description of the zero-field experiment can be obtained by treating $(\mathcal{Z}_x, \mathcal{Z}_y, \mathcal{Z}_z)$ as a pseudospin that precesses about different axes during the pulse and the detection period.

We assume that the scalar order is represented by a term in the density matrix proportional to $\mathbf{S}\cdot\mathbf{I}$, and we simplify notation by neglecting the proportionality constant and writing

$$\rho_1 = \mathbf{S}\cdot\mathbf{I} = \mathcal{Z}_z + S_z I_z. \tag{32}$$

The Hamiltonian for the pulse applied along the laboratory-frame z axis is

$$H_{\rm dc} = -B_z(\gamma_I I_z + \gamma_S S_z), \tag{33}$$

where the notation has been chosen to highlight the fact that a dc pulse rather than a conventional rf pulse is applied. The pulse has been assumed to be sufficiently short that the evolution associated with the scalar coupling can be neglected. We write the pulse Hamiltonian in the form

$$\begin{aligned} H_{\rm dc} = &-\frac{B_z}{2}(\gamma_I + \gamma_S)(I_z + S_z) \\ &-\frac{B_z}{2}(\gamma_I - \gamma_S)(I_z - S_z) \end{aligned} \tag{34}$$

and note that the operator $(I_z + S_z)$ in the first line of Eq. (34) does not contribute to the evolution of the density matrix, since it commutes with ρ_1 as well as with $(I_z - S_z)$. Dropping the term proportional to $(I_z + S_z)$ and defining

$$\omega_1 = -B_z(\gamma_I - \gamma_S) \tag{35}$$

gives

$$H_{\rm dc} = \frac{\omega_1}{2}(I_z - S_z) \tag{36a}$$

$$= \omega_1 \mathcal{Z}_x. \tag{36b}$$

A further simplification is possible because the operator $S_z I_z$ of Eq. (32) commutes with $H_{\rm dc}$ as well as with H_J, which governs the detection period that follows the pulse. Since it commutes with both of these Hamiltonians, the term $S_z I_z$ does not evolve coherently during the experiment or contribute to the signal. We can therefore replace Eq. (32) by

$$\rho_1 = \mathcal{Z}_z. \tag{37}$$

Equations (36b) and (37) present a simple picture of the evolution during the pulse: a pseudospin initially polarized along the $\tilde{z}$ axis precesses about a static field colinear with the $\tilde{x}$ axis. After the pseudospin has precessed for time t, the density matrix is

$$\rho(t) = \mathcal{Z}_z\cos(\omega_1 t) - \mathcal{Z}_y\sin(\omega_1 t).$$

Figure 4(b) depicts this evolution. As shown in the figure, a pulse that rotates the pseudospin through an angle of $\pi/2$ converts the density matrix ρ_1 to

$$\rho_2 = -\mathcal{Z}_y. \tag{38}$$

This rotation corresponds to a pulse satisfying $\omega_1\tau = \pi/2$, where τ is the pulse length.

To visualize the evolution that occurs during the ensuing detection period, we write the scalar-coupling Hamiltonian as

$$H_J = 2\pi J_{SI}\,\mathcal{Z}_z + 2\pi J_{SI}\,S_z I_z. \tag{39}$$

In Eq. (39), the operators $S_z I_z$ and $\mathcal{Z}_z$ commute, and since $S_z I_z$ also commutes with ρ_2, we can make the simplification

$$H_J = 2\pi J_{SI}\,\mathcal{Z}_z. \tag{40}$$

Equations (38) and (40) show that the evolution during the detection period can be visualized as precession about the $\tilde{z}$

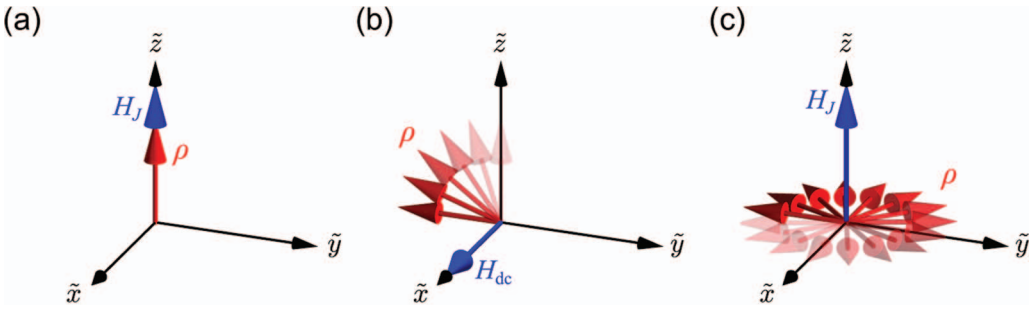

FIG. 4. Depiction of the evolution occurring in a two-spin system during the pulse and the detection period. Expressing the density matrix ρ and the Hamiltonians H_J and H_{dc} in terms of the Cartesian components of a pseudospin yields a simple model of the evolution. The axes of the pseudospin are distinguished from the laboratory-frame axes by the labels $\tilde{x}$, $\tilde{y}$, and $\tilde{z}$. (a) Just before the pulse, the pseudospin that represents the polarized system is colinear with H_J. (b) The pulse Hamiltonian is perpendicular to H_J, and the pulse rotates the pseudospin through an angle of $\pi/2$. (c) Free evolution during the detection period corresponds to precession of the pseudospin about H_J. This precession is associated with a periodic exchange between I_z and S_z, which produces an oscillating magnetization in the sample, since the spins have different gyromagnetic ratios.

axis, starting from a state polarized along $-\tilde{y}$. With relaxation neglected, the density matrix is

$$\rho(t) = -\mathcal{Z}_y \cos(\omega t) + \mathcal{Z}_x \sin(\omega t) \tag{41}$$

during the detection period, where $\omega = 2\pi J_{SI}$, and where $t = 0$ is chosen to correspond to the end of the pulse. Figure 4(c) depicts this evolution.

Physically, the pulse causes the transverse components of I and S to precess at different frequencies. As a result, the angle between the transverse components of the two nuclei changes at frequency ω_1 during the pulse. A $\pi/2$ pulse thus converts $S_xI_x + S_yI_y$ into $S_xI_y - S_yI_x$. Although this spin order is not directly detectable, it evolves under the scalar-coupling Hamiltonian to have the form $\pm(I_z - S_z)/2$, which represents sample magnetization, since the gyromagnetic ratios of the two spins are different. Continuing evolution causes a periodic exchange between I_z and S_z, with $\pm(S_xI_y - S_yI_x)$ functioning as an intermediate state in the exchange. This periodic exchange produces an oscillating magnetization in the sample, represented in Eq. (41) by the term

$$\mathcal{Z}_x \sin(\omega t) = \frac{1}{2}(I_z - S_z)\sin(\omega t).$$

The use of a short dc pulse to convert scalar order to vector order for detection in a zero-field environment can be distinguished from the ALTADENA experiment, where the sample is transported adiabatically to high field before detection.[3] Adiabatic transport from zero field to a strong magnetic field directed along the z axis transforms the density matrix ρ_1 of Eq. (32) to

$$\rho_{high} = S_zI_z \mp \frac{1}{2}(I_z - S_z). \tag{42}$$

In Eq. (42), the minus sign corresponds to the case where J_{SI} and $(\gamma_I - \gamma_S)$ have the same sign, while the plus sign corresponds to the opposite case.[3] The term $(I_z - S_z)/2$ in Eq. (42) represents sample magnetization. An oscillating signal can be generated by applying an rf pulse to either nucleus or to both nuclei. Note that when S represents a ^{13}C nucleus coupled to ^{1}H through a single bond, adiabatic transport from zero field to Earth's field ($\sim$50 μT) yields the density matrix ρ_{high} to a good approximation, since the difference between the Larmor frequencies of ^{1}H and ^{13}C in Earth's field ($\sim$1.5 kHz) is roughly an order of magnitude larger than characteristic single-bond couplings between ^{1}H and ^{13}C.

B. *N*-spin system

1. Pseudospin model

In analyzing the evolution that occurs during the dc pulse in the zero-field experiment, we view the system of N spins 1/2 as a collection of two-spin systems, each containing S as well as a single spin I that corresponds to one of the manifolds of proton angular momentum. The evolution of these two-spin systems during the pulse can be described using a generalization of the two-spin model presented in Sec. III A.

The arguments used to derive Eq. (36a) show that the pulse Hamiltonian can be written in the form

$$H_{dc} = \frac{\omega_1}{2}(I_z - S_z), \tag{43}$$

where ω_1 is given by Eq. (35), and where the spin component I_z is summed over the protons. Equation (43) implies that the transverse components of I and S precess in opposite directions during the pulse, each at frequency $\omega_1/2$, which causes the angle between the transverse components to be modulated at frequency ω_1.

We consider first the three-spin system with one strong coupling, which is discussed in detail in Sec. II B 2. In basis B_1, given by Eq. (17), the 8×8 pulse Hamiltonian is block diagonal and can be written as

$$H_{dc} = \begin{bmatrix} \omega_1/4 & & & \\ & H_{dc}^{(+1/2)} & & \\ & & H_{dc}^{(-1/2)} & \\ & & & -\omega_1/4 \end{bmatrix}, \tag{44}$$

where the 3×3 submatrices $H_{dc}^{(+1/2)}$ and $H_{dc}^{(-1/2)}$ represent the restriction of H_{dc} to the eigenspaces of F_z with eigenvalues $M_F = +1/2$ and $M_F = -1/2$, respectively:

$$H_{dc}^{(\pm 1/2)} = \frac{\omega_1}{2}\begin{bmatrix} \pm 1/6 & 2\sqrt{2}/3 & 0 \\ 2\sqrt{2}/3 & \pm 5/6 & 0 \\ 0 & 0 & \mp 1/2 \end{bmatrix}. \tag{45}$$

Two symmetries of the pulse Hamiltonian are responsible for its block-diagonal form in this basis. First, H_{dc} is the z component of a vector operator, and so the Wigner-Eckart theorem implies that when expressed in a basis of states $|F, M_F\rangle$, it can have nonzero matrix elements only between states that have the same value of M_F. Second, H_{dc} induces a uniform rotation of the protons, and so it does not couple states derived from different manifolds of the proton angular momentum I. As a result of these two symmetries, the only nonzero off-diagonal elements of H_{dc} are between pairs of states,

$$|F = 3/2, M_F, I = 1\rangle,$$
$$|F = 1/2, M_F, I = 1\rangle,$$

where M_F is $+1/2$ or $-1/2$.

For the N-spin system, the same two symmetries simplify the matrix for H_{dc} in basis B_1, which is obtained by adding the angular momentum $S = 1/2$ to manifolds of the proton angular momentum I. In general, adding S to a manifold of I yields two manifolds X_1 and X_2. The pulse Hamiltonian couples states belonging to X_1 and X_2, since they are derived from the same manifold of I, but X_1 and X_2 are not coupled by the pulse to any of the other manifolds associated with basis B_1. From the Wigner-Eckart theorem, states coupled by H_{dc} have the same value of M_F and can thus be represented as pairs

$$\begin{aligned} |a\rangle &= |F = (I + 1/2), M_F, I\rangle, \\ |b\rangle &= |F = (I - 1/2), M_F, I\rangle. \end{aligned} \tag{46}$$

It follows that the states of B_1 can be ordered such that H_{dc} is a block-diagonal matrix with 1×1 and 2×2 blocks along the diagonal, as in Eqs. (44) and (45).

Single-transition operators can be used to describe the pulse evolution in the space spanned by a pair of states $|a\rangle$, $|b\rangle$. In Eq. (45), for example, the 2×2 block in $H_{dc}^{(+1/2)}$ can be written as

$$\omega_1 \left(\frac{1}{4} + \frac{2\sqrt{2}}{3} \mathcal{Z}_x - \frac{1}{3} \mathcal{Z}_z \right),$$

where

$$\mathcal{Z}_x = \frac{1}{2} \begin{bmatrix} 0 & 1 \\ 1 & 0 \end{bmatrix},$$
$$\mathcal{Z}_z = \frac{1}{2} \begin{bmatrix} 1 & 0 \\ 0 & -1 \end{bmatrix}$$

are single-transition operators that can be identified with components of a pseudospin. More generally, the restriction of H_{dc} to the space spanned by states $|a\rangle$ and $|b\rangle$ of Eq. (46) is

$$H_{dc} = \omega_1 \left[\frac{M_F}{2} + \frac{\sqrt{(2I+1)^2 - 4M_F^2}}{2I+1} \mathcal{Z}_x - \frac{2M_F}{2I+1} \mathcal{Z}_z \right]. \tag{47}$$

Equation (47) shows that the evolution during the pulse can be visualized as precession of pseudospins at frequency ω_1, since the coefficients of $\mathcal{Z}_x$ and $\mathcal{Z}_z$ define a unit vector. Note that Eq. (36b), which holds for the two-spin system, is a special case of Eq. (47).

For a description of the physical evolution occurring in these two-dimensional subspaces, we first note that the states $|a\rangle$ and $|b\rangle$ of Eq. (46) are linear combinations of product states $|I, M_I\rangle|S, M_S\rangle$, where M_I and M_S are eigenvalues of I_z and S_z, respectively. In particular, $|a\rangle$ and $|b\rangle$ are linear combinations of the states

$$\begin{aligned} |c\rangle &= |I, M_I = M_F - 1/2\rangle \, |S, M_S = 1/2\rangle, \\ |d\rangle &= |I, M_I = M_F + 1/2\rangle \, |S, M_S = -1/2\rangle. \end{aligned}$$

Precession of I and S in opposite directions causes $|c\rangle$ and $|d\rangle$ to accumulate phase at frequencies $\omega_1(M_F - 1)/2$ and $\omega_1(M_F + 1)/2$, respectively. Changes in the relative phase of $|c\rangle$ and $|d\rangle$ correspond to transitions between $|a\rangle$ and $|b\rangle$. In Eq. (47), the $\mathcal{Z}_x$ component of the pulse Hamiltonian characterizes the rate at which these transitions occur. A complete description of the pulse evolution must also take account of the fact that the relative phase of $|a\rangle$ and $|b\rangle$ is modulated by the precession of I and S, as well as the fact that phase differences develop between states belonging to different subspaces. Modulation of the relative phase of $|a\rangle$ and $|b\rangle$ is associated with the $\mathcal{Z}_z$ component of the pulse Hamiltonian, while the term proportional to the identity in Eq. (47) contributes to phase differences between subspaces.

2. Evolution of the density matrix

The pseudospin model simplifies the description of the pulse evolution by exploiting the fact that the H_{dc} induces a uniform rotation of the protons, and analysis based on this model requires a switch from the energy eigenbasis to a basis in which I is a good quantum number. We illustrate the significance of this change of basis with calculations performed for the three-spin system that has one strong coupling. In particular, we evaluate the coherences excited by a $\pi/2$ pulse, that is, a pulse satisfying $\omega_1 \tau = \pi/2$, where ω_1 is given by Eq. (35) and τ is the pulse length.

In the energy eigenbasis B_2, defined in the paragraph containing Eq. (17), the density matrix ρ_1 representing the scalar order of the polarized system is specified by Eq. (21):

$$\rho_1^{(+1/2)} = \rho_1^{(-1/2)} = \frac{1}{2} \begin{bmatrix} 0 & 0 & 0 \\ 0 & 3/4 & 0 \\ 0 & 0 & 1/4 \end{bmatrix}.$$

In order to describe the pulse evolution using the pseudospin model, we transform ρ_1 to basis B_1, which gives

$$\rho_1^{(+1/2)} = \rho_1^{(-1/2)} = \frac{1}{2} \begin{bmatrix} 0 & 0 & 0 \\ 0 & 3/8 & -\sqrt{3}/8 \\ 0 & -\sqrt{3}/8 & 5/8 \end{bmatrix}. \tag{48}$$

Equation (48) can be compared with the form of the pulse Hamiltonian in basis B_1, given by Eqs. (44) and (45). On the right side of Eq. (48), the element in position (2, 2) is associated with a pseudospin that is aligned with the negative $\tilde{z}$ axis. The pseudospin precesses about an effective field during the pulse. The matrix element in position (3, 3) does not change

during the pulse. The off-diagonal elements of $\rho_1^{(\pm 1/2)}$ are associated with operators $|\phi\rangle\langle\psi|$ for which the bra and the ket "evolve in different spaces." To follow the evolution of the element in position (2, 3), for instance, we must consider a ket $|\phi\rangle$ that precesses as a pseudospin during the pulse and a bra $\langle\psi|$ that simply accumulates phase.

To see why the transformation from basis B_2 to basis B_1 is needed for analysis of the pulse, consider the matrix obtained by expressing $H_{\rm dc}^{(\pm 1/2)}$ in basis B_2:

$$H_{\rm dc}^{(\pm 1/2)} = \frac{\omega_1}{2}\begin{bmatrix} \pm 1/6 & -\sqrt{2}/3 & -\sqrt{2/3} \\ -\sqrt{2}/3 & \mp 1/6 & \pm 1/\sqrt{3} \\ -\sqrt{2/3} & \pm 1/\sqrt{3} & \pm 1/2 \end{bmatrix}. \tag{49}$$

Qualitative analysis of the evolution associated with Eq. (49) is not straightforward, and for larger spin systems, the problem of understanding the pulse evolution in the energy eigenbasis becomes intractable.

Evaluating the evolution of the density matrix in basis B_1, we find that a $\pi/2$ pulse yields

$$\rho_2^{(\pm 1/2)} = \frac{1}{2}\begin{bmatrix} \frac{1}{6} & \frac{\pm 1-3i}{12\sqrt{2}} & \frac{\pm 1+i}{4\sqrt{6}} \\ \frac{\pm 1+3i}{12\sqrt{2}} & \frac{5}{24} & \frac{-1\pm 2i}{8\sqrt{3}} \\ \frac{\pm 1-i}{4\sqrt{6}} & \frac{-1\mp 2i}{8\sqrt{3}} & \frac{5}{8} \end{bmatrix},$$

where ρ_2 is the density matrix that represents the system at the end of the pulse. To find the coherences excited by the pulse, we transform ρ_2 to the energy eigenbasis B_2:

$$\rho_2^{(\pm 1/2)} = \frac{1}{2}\begin{bmatrix} \frac{1}{6} & \frac{\pm 1+3i}{12\sqrt{2}} & \frac{\mp 1+i}{4\sqrt{6}} \\ \frac{\pm 1-3i}{12\sqrt{2}} & \frac{7}{12} & \frac{-1\pm i}{4\sqrt{3}} \\ \frac{\mp 1-i}{4\sqrt{6}} & \frac{-1\mp i}{4\sqrt{3}} & \frac{1}{4} \end{bmatrix}. \tag{50}$$

The off-diagonal terms in Eq. (50) represent coherences that oscillate during the detection period.

3. Development of vector order

The pulse Hamiltonian is the z component of a vector operator, and spin order of the form T_0^k can therefore develop within the molecule during the pulse, where

$$T_{-k}^k, T_{-k+1}^k, \ldots, T_k^k$$

denote the components of an arbitrary spherical tensor operator of rank k. Since detectable spin order takes the form of magnetization, which transforms as a vector under rotations, we are concerned with the development of vector order, defined formally as spin order represented by a spherical tensor operator of rank $k = 1$.

We first show that the pulse causes vector order of the form T_0^1 to develop in the three-spin system that has one strong coupling. We let V represent the z component of an arbitrary Hermitian vector operator for this system. The Wigner-Eckart theorem implies that when V is expressed in basis B_1 or B_2, it is block diagonal and has the form

$$V = \begin{bmatrix} \frac{3}{2}c_1 & & & \\ & V^{(+1/2)} & & \\ & & V^{(-1/2)} & \\ & & & -\frac{3}{2}c_1 \end{bmatrix}, \tag{51}$$

where

$$V^{(\pm 1/2)} = \begin{bmatrix} \pm\frac{1}{2}c_1 & d_1 & d_2 \\ d_1^* & \pm\frac{1}{2}c_2 & \pm d_3 \\ d_2^* & \pm d_3^* & \pm\frac{1}{2}c_3 \end{bmatrix}, \tag{52}$$

with c_n real and d_n complex. Note that setting each c_n to 1 and each d_n to zero gives $V = F_z$.

Just as Eqs. (28) and (29) implicitly express an arbitrary Hermitian scalar operator A as a linear combination of scalar operators, Eqs. (51) and (52) implicitly express V as a linear combination of operators that transform as the z component of a vector. By projecting ρ_2 onto the space spanned by these operators, we can eliminate terms from the density matrix that do not represent vector order. Performing this projection for the density matrix of Eq. (50), we obtain an expression for the vector order present at the end of the pulse:

$$\rho_2^{(\pm 1/2)} = \frac{i}{2}\begin{bmatrix} 0 & \frac{1}{4\sqrt{2}} & \frac{1}{4\sqrt{6}} \\ -\frac{1}{4\sqrt{2}} & 0 & \pm\frac{1}{4\sqrt{3}} \\ -\frac{1}{4\sqrt{6}} & \mp\frac{1}{4\sqrt{3}} & 0 \end{bmatrix}. \tag{53}$$

In Sec. IV, we show that this vector order gives rise to oscillating magnetization during the period of free evolution that follows the pulse.

More generally, the development of vector order during the pulse can be described analytically. Consider as an example the general three-spin system polarized by NH-PHIP. The discussion in Sec. II C shows that when expressed in basis B_1, the density matrix ρ_1 has the form

$$\rho_1 = \begin{bmatrix} a_1 & & & \\ & \rho_1^{(+1/2)} & & \\ & & \rho_1^{(-1/2)} & \\ & & & a_1 \end{bmatrix}, \tag{54}$$

where

$$\rho_1^{(+1/2)} = \rho_1^{(-1/2)} = \begin{bmatrix} a_1 & 0 & 0 \\ 0 & a_2 & a_4 \\ 0 & a_4 & a_3 \end{bmatrix}, \tag{55}$$

with a_n real. To describe the development of vector order during the pulse, we start from an initial state that has a single nonzero coefficient $a_n = 1$ in Eqs. (54) and (55). We solve the equation of motion analytically, retaining only the terms that correspond to vector order, as determined by Eqs. (51) and (52). Letting V_n represent the vector order that develops from the initial state which has $a_n = 1$, we find that each V_n evolves sinusoidally at frequency ω_1 during the pulse, achieving its maximum magnitude at times t for which

$$\omega_1 t = \pm\frac{\pi}{2}, \pm\frac{3\pi}{2}, \ldots. \tag{56}$$

In particular,

$$V_n = \begin{bmatrix} 0 & & & \\ & V_n^{(+1/2)} & & \\ & & V_n^{(-1/2)} & \\ & & & 0 \end{bmatrix},$$

where

$$V_1^{(\pm 1/2)} = i \sin(\omega_1 t) \begin{bmatrix} 0 & \frac{\sqrt{2}}{3} & 0 \\ -\frac{\sqrt{2}}{3} & 0 & 0 \\ 0 & 0 & 0 \end{bmatrix}, \tag{57a}$$

$$V_2^{(\pm 1/2)} = i \sin(\omega_1 t) \begin{bmatrix} 0 & -\frac{\sqrt{2}}{3} & 0 \\ \frac{\sqrt{2}}{3} & 0 & 0 \\ 0 & 0 & 0 \end{bmatrix}, \tag{57b}$$

$$V_3^{(\pm 1/2)} = 0, \tag{57c}$$

$$V_4^{(\pm 1/2)} = i \sin(\omega_1 t) \begin{bmatrix} 0 & 0 & -\frac{\sqrt{2}}{3} \\ 0 & 0 & \mp\frac{2}{3} \\ \frac{\sqrt{2}}{3} & \pm\frac{2}{3} & 0 \end{bmatrix}. \tag{57d}$$

Note that the vector order of Eqs. (57a) and (57b) corresponds to polarization of pseudospins along $\pm\tilde{y}$, which evolves from scalar order represented by pseudospins aligned with $\pm\tilde{z}$. A similar result was obtained in Sec. III A for the two-spin system. For Eq. (57d), the initial scalar order is not contained within the 2×2 spaces where the pseudospins are defined, and the development of vector order involves a bra and a ket that "evolve in different spaces."

The approach used to derive Eqs. (57a) through (57d) can be generalized to the N-spin system. In basis B_1, the density matrix ρ_1 can be expanded as a linear combination of scalar operators A_n, A'_{jk}, as discussed in Sec. II C. Since $H_{\rm dc}$ has only 1×1 and 2×2 blocks along the diagonal, with the 2×2 blocks given by Eq. (47), the evolution during the pulse can be evaluated analytically when the initial state is A_n or A'_{jk}. The evolution is confined to low-dimensional spaces, within which the structure of the relevant vector order can be explicitly described, as in Eqs. (51) and (52). The vector order that develops from A_n or A'_{jk} is found to be a matrix of imaginary numbers proportional to $\sin(\omega_1 t)$, as in Eqs. (57a), (57b) and (57d). For an initial state A_n, the scalar order present at the beginning of the pulse is represented by pseudospins aligned with $\pm\tilde{z}$, and the vector order that develops during the pulse corresponds to polarization along $\pm\tilde{y}$.

As shown in Appendix A, the states of the energy eigenbasis B_2 can be chosen as real linear combinations of the states in basis B_1. Transforming the terms in the density matrix that represent vector order from basis B_1 to basis B_2 therefore yields a matrix of imaginary numbers proportional to $\sin(\omega_1 t)$. It follows that for the N-spin system, the vector order introduced by the pulse consists of a set of imaginary-valued coherences, as in Eq. (53). A pulse that rotates the transverse components of I through an angle of $\pm\pi/2$ relative to those of S is optimal for excitation of these coherences. Consistent with this theoretical result, a pulse length τ satisfying $\omega_1 \tau = \pi/2$ was found to give optimal signal intensity in zero-field experiments where pyridine-^{15}N was polarized by means of NH-PHIP.[31]

IV. EVOLUTION OF THE VECTOR ORDER

During the period of free evolution that follows the pulse, the vector order evolves as a set of oscillating coherences. Since the Hamiltonian H_J is a scalar operator, the symmetry of the spin order under rotations does not change during the evolution. Formally, the vector order present at the end of the pulse consists of tensor operators of form T_0^1, as noted in Sec. III B 3, and this form is preserved during the evolution.

The zero-field spectrum is obtained by detecting the sample magnetization during the evolution period and then taking the Fourier transform. Since magnetization along x or y would be associated with spin order of the form $T_{\pm 1}^1$, which is not present, magnetization can only develop along the z axis. We therefore define the observable as

$$\mu_z = \gamma_I \hbar I_z + \gamma_S \hbar S_z,$$

the z component of the molecular spin dipole.

Like the pulse Hamiltonian $H_{\rm dc}$, the operator μ_z can be decomposed as a linear combination of the operators $(I_z - S_z)$ and $(I_z + S_z)$. Since H_J commutes with the total angular momentum, the term proportional to $(I_z + S_z)$ does not contribute to the oscillating signal. Dropping this term gives

$$\mu_z = \frac{\hbar}{2}(\gamma_I - \gamma_S)(I_z - S_z). \tag{58}$$

In showing how the evolution under H_J causes oscillations in $\langle \mu_z \rangle$, we consider a pair of angular-momentum manifolds that have distinct spin energies and are coupled by the operator μ_z. Since $H_{\rm dc} \propto \mu_z$, the pulse induces transitions between the two manifolds and causes coherences to develop. We consider the case where these coherences represent vector order. Immediately after the pulse, the coherences have imaginary values, as noted in Sec. III B 3, and they evolve to have real values after a time period $t = \pi/4\omega$, where ω is the oscillation frequency determined by the energy difference between the manifolds. Appendix A shows that the matrix elements of μ_z can be assumed real in the energy eigenbasis; in particular, the matrix elements of μ_z that couple the two manifolds represent the z component of a real vector operator. Since the coherences present at time $t = \pi/4\omega$ also represent the z component of a real vector operator, the Wigner-Eckart theorem implies that these coherences are related by a proportionality constant to the matrix elements of μ_z that couple the two manifolds. If we neglect the proportionality constant, the real parts of the oscillating coherences can then be identified with matrix elements of μ_z, while the imaginary parts must correspond to undetectable vector order. The oscillating real parts thus represent a contribution to $\langle \mu_z(t) \rangle$, and this contribution appears in the spectrum as a peak at frequency ω.

Physically, the evolution of the vector order induces a periodic exchange between I_z and S_z, with undetectable spin order functioning as an intermediate state during the exchange.

Since the gyromagnetic ratios for I and S are different, the exchange between I_z and S_z produces an oscillating magnetization, which constitutes the NMR signal. In general, each pair of manifolds that can be coupled by a vector operator yields a spectral peak, which gives the selection rule $\Delta F = 0, \pm 1$.

We use the two-spin system introduced in Sec. III A to illustrate these conclusions. At the end of the pulse, the vector order has the form

$$S_x I_y - S_y I_x = \frac{1}{2}\begin{bmatrix} 0 & i \\ -i & 0 \end{bmatrix}, \tag{59}$$

where the right side of Eq. (59) is obtained by expressing the operator in the two-dimensional space spanned by the energy eigenstates $|F = 1, M_F = 0\rangle$ and $|F = 0, M_F = 0\rangle$. Note that the undetectable order represented by Eq. (59) is the imaginary part of a coherence. The real part is

$$\frac{1}{2}(I_z - S_z) = \frac{1}{2}\begin{bmatrix} 0 & 1 \\ 1 & 0 \end{bmatrix}, \tag{60}$$

which is proportional to the observable μ_z of Eq. (58). As the coherence evolves under H_J, it alternates between real and imaginary values, which corresponds to conversion of the spin order between the forms represented by Eqs. (59) and (60). Oscillations in the real part of the coherence yield a signal.

For the three-spin system that has one strong coupling, the spin order present at the end of the polarization period is given by Eq. (22) as

$$-\frac{1}{4}(\mathbf{S} + \mathbf{I}_1) \cdot \mathbf{I}_2,$$

where the term proportional to the identity has been dropped. Since the pulse induces a uniform rotation of the two protons, the term $\mathbf{I}_1 \cdot \mathbf{I}_2$ does not evolve during the pulse, remaining instead in the form of undetectable scalar order. The relevant scalar order of the polarized system is thus

$$\rho_1 = -\frac{1}{4}\mathbf{S} \cdot \mathbf{I}_2.$$

A $\pi/2$ pulse converts ρ_1 to

$$-\frac{1}{4}(S_z I_{2z} + S_x I_{2y} - S_y I_{2x}).$$

Arguments similar to those used to derive Eq. (53) from Eq. (50) show that $S_z I_{2z}$ does not contribute to the vector order present at the end of the pulse, which is given by

$$\rho_2 = -\frac{1}{4}(S_x I_{2y} - S_y I_{2x}).$$

This vector order is associated with a set of imaginary-valued coherences between states belonging to different manifolds, as shown by Eq. (53), which expresses ρ_2 in the energy eigenbasis B_2. During the detection period, the real parts of the coherences represent oscillations in $\langle \mu_z(t) \rangle$.

To find the spectrum of $\langle \mu_z(t) \rangle$ for this system, we first note that the coherences responsible for dipole oscillations are represented by the evolving density matrix

$$\rho(t) = \exp(-it H_J)\, \rho_2\, \exp(it H_J),$$

where time $t = 0$ has been chosen to correspond to the beginning of the detection period. In basis B_2, this density matrix takes the form

$$\rho = \begin{bmatrix} 0 & & & \\ & \rho^{(+1/2)} & & \\ & & \rho^{(-1/2)} & \\ & & & 0 \end{bmatrix},$$

where

$$\rho^{(\pm 1/2)} = \frac{i}{2}\begin{bmatrix} 0 & \frac{1}{4\sqrt{2}}e^{-i\omega_{12}t} & \frac{1}{4\sqrt{6}}e^{-i\omega_{13}t} \\ -\frac{1}{4\sqrt{2}}e^{i\omega_{12}t} & 0 & \pm\frac{1}{4\sqrt{3}}e^{-i\omega_{23}t} \\ -\frac{1}{4\sqrt{6}}e^{i\omega_{13}t} & \mp\frac{1}{4\sqrt{3}}e^{i\omega_{23}t} & 0 \end{bmatrix}.$$

The transition frequencies ω_{jk} can be evaluated using Table II:

$$\begin{aligned} \omega_{12}/2\pi &= \frac{3}{4}(J_{S2} + J_{12}), \\ \omega_{13}/2\pi &= J_{S1} + \frac{1}{4}(J_{S2} + J_{12}), \\ \omega_{23}/2\pi &= J_{S1} - \frac{1}{2}(J_{S2} + J_{12}). \end{aligned} \tag{61}$$

Expressing μ_z in basis B_2 and setting to zero its diagonal elements, which do not contribute to the signal, we obtain

$$\mu_z^{(\pm 1/2)} = \frac{\hbar}{2}(\gamma_I - \gamma_S)\begin{bmatrix} 0 & -\frac{\sqrt{2}}{3} & -\sqrt{\frac{2}{3}} \\ -\frac{\sqrt{2}}{3} & 0 & \pm\frac{1}{\sqrt{3}} \\ -\sqrt{\frac{2}{3}} & \pm\frac{1}{\sqrt{3}} & 0 \end{bmatrix}.$$

The oscillating spin dipole is given by

$$\langle \mu_z(t) \rangle = \mathrm{Tr}\{\mu_z \rho(t)\},$$

which evaluates to

$$\begin{aligned} \langle \mu_z(t) \rangle = &-\frac{\hbar}{12}(\gamma_I - \gamma_S) \\ &\times [\sin(\omega_{12}t) + \sin(\omega_{13}t) - \sin(\omega_{23}t)]. \end{aligned} \tag{62}$$

Taking the Fourier transform of this signal yields an imaginary spectrum, which is a general feature of signals enhanced by PHIP or NH-PHIP at zero magnetic field. The scalar order represented by ρ_1 has no dipole moment, and $\langle \mu_z \rangle$ does not evolve during the pulse, since μ_z commutes with the pulse Hamiltonian. It is only during the evolution under H_J that a dipole moment develops. Since the vector order present at the beginning of the detection period corresponds to a set of imaginary-valued coherences, each oscillating component of $\langle \mu_z(t) \rangle$ is equal to zero at time $t = 0$, which implies an imaginary spectrum. In Appendix A, we show that the same conclusion can be established using symmetry arguments.

The signal given by Eq. (62) has a spectrum with equal-amplitude peaks at the three transition frequencies of the system, including an antiphase doublet at $\sim J_{S1}$. This doublet can be seen in Fig. 5, which shows experimental and simulated spectra for hyperpolarized dimethyl maleate obtained by adding parahydrogen to dimethyl acetylenedicarboxylate, a reaction shown in Fig. 1. The methods used for the experiment and for the simulations have been described in Ref. 12. With ^{13}C at natural abundance, the reaction yields a mixture of isotopomers that correspond to different positions of the ^{13}C nucleus. As noted in the introduction to Sec. II, the

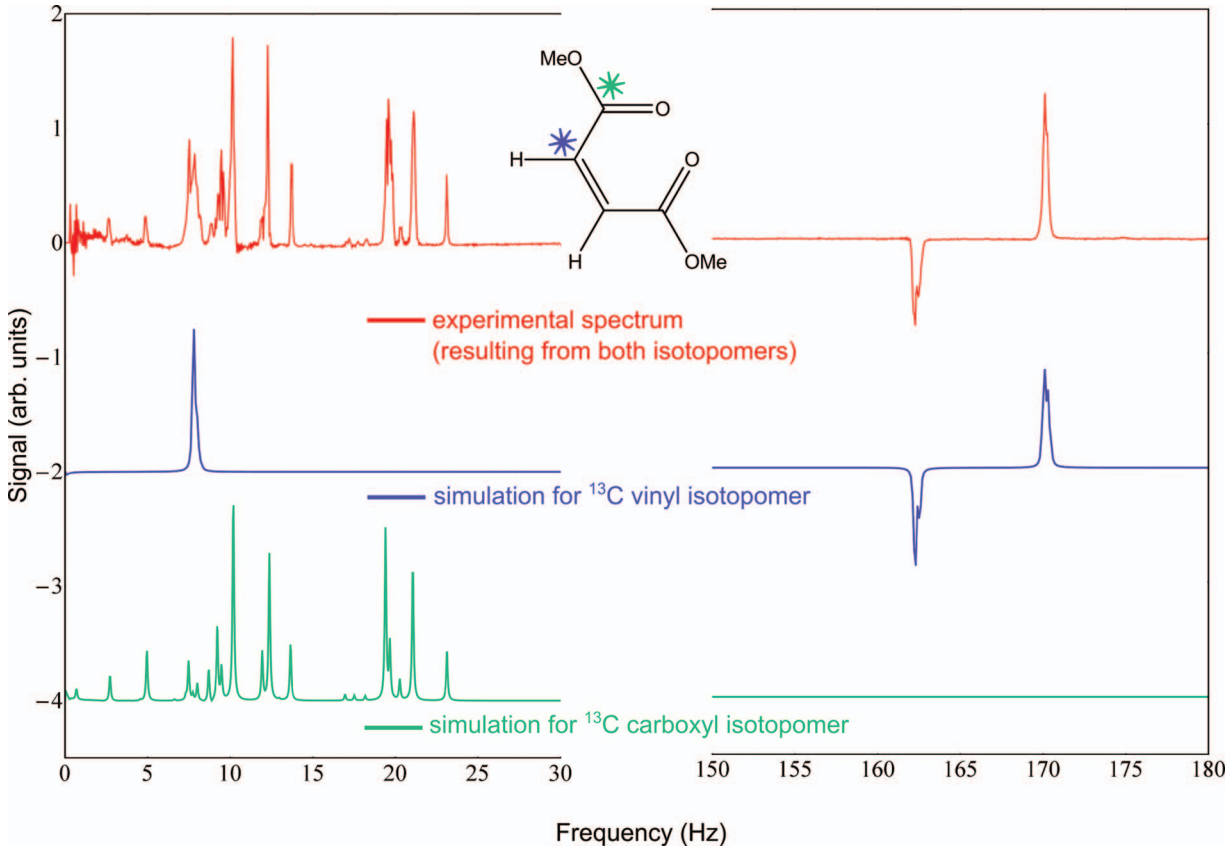

FIG. 5. Zero-field spectrum resulting from the addition of parahydrogen to dimethyl acetylenedicarboxylate to form dimethyl maleate. Below the experimental spectrum are simulations for the two isotopomers that contribute to the signal. The spectra have been phased so that the low-frequency peaks appear above the horizontal axis. For the vinyl isotopomer, the spectrum has the form predicted by Eq. (62), which was derived by modeling the isotopomer as a three-spin system. In particular, there are peaks of equal integrated area at the frequencies $\omega_{jk}/2\pi$, including a pair of antiphase peaks at $\sim J_{S1}$. The small splittings of the antiphase peaks are due to weak couplings to the methyl protons, which are not included in the three-spin model. The coupling constants used in the simulation of the vinyl isotopomer were $^1J_{S1} = 167.2$ Hz, $^2J_{S2} = -2.2$ Hz, $^3J_{12} = 13.0$ Hz, $^4J_{S3} = -0.45$ Hz, $^5J_{13} = 0.15$ Hz, and $^6J_{23} = 0$ Hz. For the carboxyl isotopomer, the coupling constants were $^2J_{S1} = 2.7$ Hz, $^3J_{S2} = 13.2$ Hz, $^3J_{12} = 11.9$ Hz, $^3J_{S3} = 4.1$ Hz, $^5J_{13} = 0.15$ Hz, and $^6J_{23} = 0$ Hz. In the notation for the coupling constants, the vinyl protons are numbered 1 and 2, the protons in the methyl group are indicated by the subscript 3, and the superscript shows the number of bonds between nuclei. The couplings were adjusted to yield a visual match to the experimental spectrum.

isotopomer with ^{13}C in the vinyl group can be modeled as a three-spin system. The simulated spectrum for this isotopomer, shown directly below the experimental spectrum, has the form specified by Eq. (62), with three peaks of equal integrated area at the frequencies $\omega_{jk}/2\pi$. The small splittings in the spectrum are due to weak couplings to the methyl protons, which are not included in the three-spin model.

The bottom trace in Fig. 5 shows the simulated spectrum for the isotopomer that has ^{13}C in the carboxyl group. The network of six coupled spins formed by the ^{13}C nucleus, the vinyl protons, and the methyl protons yields a complicated splitting pattern in the low-frequency region of the spectrum. The isotopomer with ^{13}C in the methyl group is not expected to make a significant contribution to the signal, since the heteronucleus is isolated from the spins of the initial singlet state. The simulation of the experiment therefore corresponds to the sum of the lower two traces.

The theoretical signal enhancement associated with zero-field PHIP can be characterized by comparing Eq. (62) to the signal that would be obtained by prepolarizing the spin system in an external field and then shuttling it into the zero-field detection region. For this experimental scheme, the alignment of the magnetization is preserved by a guiding field as the sample is moved to the detection region; when the sample is in place, the guiding field is turned off suddenly to allow for detection in a zero-field environment.[14,16] In the simplest acquisition protocol, $\langle \mu_z(t) \rangle$ is detected during a period of free evolution that begins immediately after the guiding field along z is turned off. Thermal equilibration in a field of magnitude B_a at temperature T gives the initial density matrix,

$$\rho_{\rm th} = \frac{1}{8}\left(1 + \frac{B_a}{k_B T}\mu_z\right),$$

where the high-temperature approximation has been used. Evaluating the trace

$$\langle \mu_z(t) \rangle = {\rm Tr}\left\{\mu_z \exp(-it H_J)\, \rho_{\rm th}\, \exp(it H_J)\right\}$$

for the three-spin system that has one strong coupling, we obtain

$$\langle \mu_z(t) \rangle = \frac{B_a \hbar^2 (\gamma_I - \gamma_S)^2}{72 k_B T} \times \left[2\cos(\omega_{12} t) + 6\cos(\omega_{13} t) + 3\cos(\omega_{23} t)\right], \quad (63)$$

where the static term has been dropped. In Eq. (63), the peak at frequency ω_{13} has the largest amplitude. The amplitude of

the corresponding peak in Eq. (62) is larger by a factor of

$$\frac{k_B T}{B_a \hbar (\gamma_I - \gamma_S)},$$

which evaluates to $\sim 10^5$ in the case where $B_a = 2\text{T}$ and $T = 300\text{K}$, with γ_I and γ_S the gyromagnetic ratio of the ^{1}H nucleus and the ^{13}C nucleus, respectively.

V. CONCLUSION

Although detection of zero-field NMR by means of field-cycling was initially demonstrated decades ago,[17] the potential of zero-field NMR has remained largely unexplored. The strong signals available from PHIP and NH-PHIP show promise for enabling applications of zero-field NMR and facilitating its development, particularly in combination with multiple-pulse sequences[32] and multidimensional methods, which play a central role in many high-field applications.

Zero-field experiments that use PHIP or NH-PHIP begin with a polarization period in which the singlet state of parahydrogen evolves into scalar spin order involving spins throughout the molecule. With the effects of relaxation neglected, the density matrix ρ_1 that describes this spin order is invariant under rotations, time translation, and time reversal, and it can be diagonalized by an energy eigenbasis that divides the state space into degenerate angular-momentum manifolds. Within each of these manifolds, the spin system is unpolarized, because of the lack of any preferred spatial direction. For experiments in which parahydrogen is added chemically to a molecule, the development of scalar order during the polarization period is determined by a set of multidimensional rotations that mix manifolds obtained by addition of angular momenta to yield degenerate manifolds of energy eigenstates. These rotations can be visualized as occurring in a space where the manifolds obtained by addition of angular momenta are identified with orthogonal axes.

A short pulse along z breaks the scalar symmetry of the spin order by rotating the transverse components of I and S through different angles. The conversion of scalar order to vector order is maximal when a $\pm\pi/2$ pulse is applied, i.e., when the transverse components of I are rotated by an angle of $\pm\pi/2$ relative to those of S. The development of vector order during the pulse can be described analytically by means of single-transition operators. The state space is divided into one-dimensional and two-dimensional subspaces that are not coupled by the pulse, and within each two-dimensional space, the evolution can be visualized as the precession of a pseudospin about an effective field. The pseudospins precess at frequency $\omega_1 = -B_z(\gamma_I - \gamma_S)$, the same frequency at which the angle between the transverse components of I and S is modulated in the laboratory frame during the pulse. With the pseudospin axes denoted by $\tilde{x}$, $\tilde{y}$, and $\tilde{z}$, polarization along $\pm\tilde{z}$ at the beginning of the pulse corresponds to scalar order, while polarization along $\pm\tilde{y}$ at the end of the pulse corresponds to vector order.

During the detection period that follows that pulse, the vector order evolves under H_J as a set of oscillating coherences. The imaginary parts of the coherences represent spin order that is not directly detectable, while the real parts can be identified with oscillating magnetization. The evolution governed by H_J causes a periodic exchange between I_z and S_z, with the undetectable order represented by the imaginary parts of the coherences functioning as an intermediate state during the exchange. Because the gyromagnetic ratios γ_I and γ_S are different, the periodic exchange between I_z and S_z yields an oscillating magnetization, which constitutes the NMR signal. The frequency components of this signal are imaginary, since the pulse does not directly induce magnetization in the sample; rather, it is free evolution under H_J that generates magnetization from the vector order present at the end of the pulse.

ACKNOWLEDGMENTS

Research was supported by the U.S. Department of Energy (DOE), Office of Basic Energy Sciences, Division of Materials Sciences and Engineering under Contract No. DE-AC02-05CH11231 [theoretical work, PHIP experiments, salaries for G. Kervern, T. Theis, P. Ganssle, J. Blanchard, A. Pines], and by the National Science Foundation (NSF) under Award No. CHE-095765 [zero-field instrumentation, salaries for M. Butler, M. Ledbetter, D. Budker, A. Pines].

APPENDIX A: CONSEQUENCES OF TIME-REVERSAL AND COMPLEX-CONJUGATION SYMMETRY

The time-reversal operator can be expressed in the form[33]

$$K = \exp(-i\pi F_y) K_0, \tag{A1}$$

where K_0 acts as the complex-conjugation operator for a state function expressed in the product-state basis. Note that since the Clebsch-Gordan coefficients are real, K_0 also acts as the complex-conjugation operator for a state function expressed in any basis of states $|F, M_F\rangle$ obtained by addition of angular momenta with the Clebsch-Gordan coefficients.

Algebraic expressions involving the antiunitary operators K and K_0 can be manipulated by means of the identities

$$K \mathbf{J} K^\dagger = -\mathbf{J} \tag{A2}$$

and

$$K_0(J_x, J_y, J_z) K_0^\dagger = (J_x, -J_y, J_z), \tag{A3}$$

where J represents the spin of an arbitrary nucleus in the system. Equation (A3), in combination with the fact that K_0 is antilinear, implies that

$$K_0 \exp(-i\pi F_y) K_0^\dagger = \exp(-i\pi F_y).$$

Since K_0 commutes with the rotation appearing in Eq. (A1), a scalar operator invariant under time reversal is also invariant under complex conjugation by K_0.

1. Scalar order

For hydrogenative PHIP, the density matrix ρ_1 is an average over evolution times t governed by the scalar-coupling Hamiltonian H_J. With normalization neglected, this average

can be written as

$$\rho_1 = \sum_t \exp(-it H_J)\, \rho_0\, \exp(it H_J). \tag{A4}$$

Since H_J and the initial density matrix

$$\rho_0 = \frac{1}{4} - \mathbf{I}_1 \cdot \mathbf{I}_2$$

are invariant under time reversal, we have

$$K\rho_1 K^\dagger = \sum_t \exp(it H_J)\, \rho_0\, \exp(-it H_J). \tag{A5}$$

Comparison of Eqs. (A4) and (A5) shows that $K\rho_1 K\dagger$ corresponds to an average in which the oscillation frequency of each coherence has been reversed in sign. Since the average over t simply eliminates oscillating terms from the density matrix, this sign reversal has no effect on ρ_1. It follows that ρ_1 commutes with K, and since it is a scalar operator, it also commutes with K_0.

For NH-PHIP, the polarization period can be modeled as an average over subperiods governed by different Hamiltonians,[5] with the molecule either bound to the complex or dissociated from it throughout each subperiod. Assuming the characteristic duration of each subperiod is long enough for all oscillating coherences to be averaged to zero, reversing the sign of oscillation frequencies has no effect on the average, and it follows that ρ_1 is invariant under time reversal. As shown in Appendix B, ρ_1 is a scalar operator, which implies that it is also invariant under complex conjugation by K_0.

For the three-spin system analyzed in Sec. II A, the coherent evolution of $\rho(t)$ is specified by Eqs. (6), (10) and (11), while ρ_1 is given by Eq. (12). The operator Γ, defined by Eq. (4) as a triple product, appears in the expansion for $\rho(t)$ but not in the expansion for ρ_1. The triple product changes sign under time reversal, while ρ_1 is invariant under the same transformation, and we show below that Γ is orthogonal to ρ_1 as a result. In contrast to ρ_1, the evolving density matrix $\rho(t)$ includes oscillating coherences; it is therefore not invariant under time reversal and in general includes a nonzero contribution from Γ.

In showing that Γ is orthogonal to ρ_1, we first expand ρ_1 as a linear combination of the orthogonal operators that make a nonzero contribution to $\rho(t)$:

$$\rho_1 = b_1 + b_2 \mathbf{I}_1 \cdot \mathbf{I}_2 + b_3 \mathbf{S} \cdot \mathbf{I}_1 + b_4 \mathbf{S} \cdot \mathbf{I}_2 + b_5 \Gamma. \tag{A6}$$

Time reversal changes the sign of Γ while leaving the other operators invariant, which gives

$$\begin{aligned} \rho_1 &= K\rho_1 K^\dagger \\ &= b_1^* + b_2^* \mathbf{I}_1 \cdot \mathbf{I}_2 + b_3^* \mathbf{S} \cdot \mathbf{I}_1 + b_4^* \mathbf{S} \cdot \mathbf{I}_2 - b_5^* \Gamma, \end{aligned} \tag{A7}$$

since K is antilinear. Equations (A6) and (A7) imply that

$$b_5 = -b_5^*. \tag{A8}$$

Note that if K were linear, we would instead have $b_5 = -b_5$, which would give the desired result $b_5 = 0$. To obtain the same result from Eq. (A8), we first rearrange the terms in Eq. (A6) to obtain

$$b_5 \Gamma = \rho_1 - (b_1 + b_2 \mathbf{I}_1 \cdot \mathbf{I}_2 + b_3 \mathbf{S} \cdot \mathbf{I}_1 + b_4 \mathbf{S} \cdot \mathbf{I}_2). \tag{A9}$$

Since Eqs. (A6) and (A7) imply that each coefficient b_n appearing on the right side of Eq. (A9) is real, it follows from (A9) that $b_5\Gamma$ is Hermitian. However, Γ must also be Hermitian, since Eq. (4) defines it as a linear combination of terms $I_{1u} I_{2v} S_w$, each of which is the tensor product of three Hermitian operators. If b_5 is nonzero, Eq. (A8) implies that it is a pure imaginary number, which would contradict that conclusion that Γ and $b_5\Gamma$ are both Hermitian. It follows that b_5 is necessarily zero, which is the desired result.

The fact that ρ_1 commutes with K_0 implies that the matrix elements of ρ_1 are real in a basis where K_0 takes the complex conjugate of matrix elements. In particular, ρ_1 is real when expressed in the basis B_1, defined for the three-spin system by Eq. (17) and for the N-spin system in Appendix B, since B_1 is obtained by addition of angular momenta using the Clebsch-Gordan coefficients. Section II C shows that ρ_1 can be expanded as a linear combination of orthogonal scalar operators that have a simple form when expressed in basis B_1. In the context of that discussion, certain terms can be eliminated from the expansion because the matrix elements of ρ_1 are real.

Section II B and Appendix B discuss the structure of the scalar order that develops during the polarization period. For hydrogenative PHIP, this scalar order is determined by the transformation from basis B_1 to basis B_2, an energy eigenbasis that diagonalizes ρ_1 and divides the state space into degenerate manifolds of F. As noted in the introduction to Sec. III, the phases and amplitudes of the peaks in a zero-field spectrum obtained using PHIP or NH-PHIP can be considered to depend on the same transformation. We show here that this transformation is formally associated with a set of multidimensional rotations.

We begin by introducing an arbitrary quantum number Y that distinguishes the manifolds formed by the states of basis B_2. A state belonging to this basis can thus be written as $|F, M_F, E, \lambda, Y\rangle$, where λ is an eigenvalue of ρ_1. Similarly, a quantum number X is used to distinguish the manifolds formed by the states of basis B_1. A state of this basis set can be written as $|F, M_F, I, X\rangle$, where I is the summed angular momentum of the protons, as defined in Eq. (1).

We wish to establish that the states $|F, M_F, E, \lambda, Y\rangle$ can be chosen as real linear combinations of the states $|F, M_F, I, X\rangle$. For arbitrary Y, we have

$$|F, M_F, E, \lambda, Y\rangle = \sum c_n\, |F, M_F, I, X_n\rangle\,, \tag{A10}$$

where the sum on the right side of the equation is over the states that have the same values of F and M_F as the state on the left side of the equation. Operating on both sides of Eq. (A10) with K_0 gives state

$$K_0\, |F, M_F, E, \lambda, Y\rangle = \sum c_n^*\, |F, M_F, I, X_n\rangle\,, \tag{A11}$$

and since K_0 commutes with $\mathbf{F}^2$, F_z, H_J, and ρ_1, this state has the same quantum numbers F, M_F, E, and λ as $|F, M_F, E, \lambda, Y\rangle$. Equation (A3), in combination with the fact that K_0 is antilinear, implies that the raising and lower operators $F_x \pm iF_y$ commute with K_0, and it follows that the set of states

$$K_0\, |F, -F, E, \lambda, Y\rangle\,, \ldots\,, K_0\, |F, +F, E, \lambda, Y\rangle$$

forms an angular-momentum manifold. Letting M_F range from $-F$ to F, we find that the linear combinations

$$\frac{1}{2}\left(|F, M_F, E, \lambda, Y\rangle + K_0\,|F, M_F, E, \lambda, Y\rangle\right) = \sum \mathrm{Re}(c_n)\,|F, M_F, I, X_n\rangle \tag{A12}$$

and

$$\frac{1}{2i}\left(|F, M_F, E, \lambda, Y\rangle - K_0\,|F, M_F, E, \lambda, Y\rangle\right) = \sum \mathrm{Im}(c_n)|F, M_F, I, X_n\rangle \tag{A13}$$

form manifolds of F which span the same space as

$$|F, M_F, E, \lambda, Y\rangle\,, \quad K_0\,|F, M_F, E, \lambda, Y\rangle\,.$$

Note that the coefficients appearing on the right side of Eqs. (A12) and (A13) are real. It follows that the eigenstates $|F, M_F, E, \lambda, Y\rangle$ can be chosen as real linear combinations of the states $|F, M_F, I, X\rangle$. We assume that the eigenstates of basis B_2 have been chosen in this way.

Expressing a state $|F, M_F, E, \lambda, Y\rangle$ as a linear combination of the states $|F, M_F, I, X\rangle$ defines a single row of a matrix R_F. The remaining rows are defined by letting Y vary, while keeping F and M_F fixed. The Wigner-Eckart theorem implies that for a given F, the matrix obtained in this way does not depend on the value of M_F, and so the set of matrices R_F can be considered to describe mixing of manifolds that have quantum numbers (F, I, X) to produce manifolds that have quantum numbers (F, E, λ, Y). The matrices R_F are real, by construction, and they can be formally associated with multidimensional rotations if the ordering of the rows is chosen such that $\det(R_F) = 1$ for each F.

2. Vector order

Under the assumption that the energy eigenstates of basis B_2 are chosen as real linear combinations of the states $|F, M_F, I, X\rangle$ in B_1, the operator K_0 acts as the complex-conjugation operator for states expressed in the basis B_2. Since μ_z, defined by Eq. (58), commutes with K_0, its matrix elements are real in this basis. In Sec. IV, we use this property of μ_z, which represents the observable during the detection period, to show that the signal is associated with the real parts of oscillating coherences.

Section IV also discusses the evolution of $\langle\mu_z(t)\rangle$ during the detection period and shows that the spectrum is imaginary. The conclusion is based on a detailed analysis of the evolution occurring during the pulse; we show here that the same conclusion can be reached using the fact that ρ_1, H_J, and $(I_z - S_z)$ commute with K_0. In carrying out this derivation, we let θ represent the "flip angle" for the pulse, i.e., the angle through which the transverse components of I are rotated with respect to the transverse components of S. In order to simplify notation, we drop the proportionality constant $\hbar(\gamma_I - \gamma_S)/2$ from the expression for the observable μ_z. The signal can then be written as

$$\langle\mu_z(t)\rangle = \mathrm{Tr}\{(I_z - S_z) \times \exp(-it\,H_J)\,\rho_2\,\exp(it\,H_J)\}, \tag{A14}$$

where

$$\rho_2 = \exp[-i(\theta/2)(I_z - S_z)] \times \rho_1\,\exp[i(\theta/2)(I_z - S_z)]. \tag{A15}$$

We wish to show that if t is replaced by $-t$ in Eq. (A14), the sign of the signal changes. We define $f(t)$ to be the function obtained by making this substitution:

$$f(t) = \mathrm{Tr}\{(I_z - S_z)\exp(it\,H_J)\,\rho_2\,\exp(-it\,H_J)\}. \tag{A16}$$

Since $f(t)$ can be identified with $\langle\mu_z(t)\rangle$ in a system governed by the Hamiltonian $-H_J$, it is real-valued. Taking the complex conjugate of Eq. (A16) therefore leaves the left side of the equation unchanged. The complex conjugate of the right side of the equation is obtained by replacing the matrix product inside the curly brackets by its complex conjugate. Since the trace is invariant under a change of basis, we can consider the trace to be evaluated in a basis where K_0 acts as the complex-conjugation operator. This assumption gives

$$f(t) = \mathrm{Tr}\{(I_z - S_z) \times \exp(-it\,H_J)K_0\rho_2K_0^\dagger\,\exp(it\,H_J)\}, \tag{A17}$$

where

$$K_0\rho_2K_0^\dagger = \exp[-i(-\theta/2)(I_z - S_z)] \times \rho_1\,\exp[i(-\theta/2)(I_z - S_z)]. \tag{A18}$$

Comparison of Eqs. (A14) and (A17) shows that replacing ρ_2 by $K_0\rho_2K_0^\dagger$ in Eq. (A14) converts $\langle\mu_z(t)\rangle$ to $f(t)$. From Eqs. (A15) and (A18), this replacement amounts to changing the sign of θ, which is equivalent to reversing the direction of the pulsed field.

Note that ρ_2 can also be transformed to $K_0\rho_2K_0^\dagger$ by rotating the coordinate system by 180° about a transverse axis, as can be seen by applying such a rotation to the right side of Eq. (A15). The function $f(t)$ can thus be identified with the signal observed in the rotated coordinate system, and it follows that $f(t) = -\langle\mu_z(t)\rangle$. The periodic signal defined by (A14) is therefore an odd function of time; its frequency components are all "sine functions" rather than "cosine functions," and its spectrum is imaginary.

APPENDIX B: SCALAR ORDER OF THE *N*-SPIN SYSTEM

In generalizing the discussion of Sec. II B 1 to the N-spin system, we first consider the case where parahydrogen is chemically added to the molecule. The summed angular momentum of the spins I_1 and I_2 in the initial singlet is denoted by

$$\mathbf{I}_{12} = \mathbf{I}_1 + \mathbf{I}_2.$$

Basis B_1 is obtained by first adding I_1 and I_2 to obtain singlet and triplet manifolds of I_{12}, and then adding the angular momenta of the remaining spins, with the heteronucleus added last. Addition of angular momenta in this order yields states $|F, M_F, I, I_{12}\rangle$, where I is the summed angular momentum of the protons. When expressed in basis B_1, the initial density

matrix ρ_0 is diagonal and has zero population in all states with $I_{12} = 1$. All states with $I_{12} = 0$ have equal nonzero population.

The structure of the scalar order that develops during the polarization period can be characterized by expressing ρ_1 in an appropriately chosen basis of energy eigenstates, denoted by B_2. Since H_J commutes with $\mathbf{F}$, the vector operator for the total angular momentum, the energy eigenstates can be grouped into degenerate angular-momentum manifolds labeled with quantum numbers (F, E). The arguments given in the paragraph containing Eq. (15) generalize to show that each degenerate manifold can be considered a linear combination of the manifolds (F, I, I_{12}) formed by the states of basis B_1. As shown by the discussion in Appendix A, the invariance of H_J under time reversal implies that the mixing of manifolds (F, I, I_{12}) to form the degenerate manifolds (F, E) can be described by rotation matrices R_F. It follows from the Wigner-Eckart theorem that the time-averaged density matrix ρ_1 is proportional to the identity within each manifold (F, E), since it is a scalar operator. In the absence of additional energy degeneracies beyond those resulting from the spherical symmetry of H_J, matrix elements between states belonging to different manifolds correspond to oscillating coherences that are averaged to zero during the polarization period. The net effect of the free evolution and the average over evolution times is thus to distribute the population that is initially contained in manifolds (F, I, $I_{12} = 0$) among the manifolds (F, E) while preserving the value of F.

When additional energy degeneracies are present, we can derive the same conclusions about the structure of ρ_1 by considering the properties of its eigenstates. Under the assumption that all oscillating coherences in the density matrix are averaged to zero during the polarization period, ρ_1 commutes with H_J, which implies that ρ_1 can be diagonalized by a set of energy eigenstates. Since ρ_1 and H_J both commute with $\mathbf{F}$, the energy eigenstates that diagonalize ρ_1 can be chosen to form degenerate manifolds of F. Since it is a scalar operator, ρ_1 is proportional to the identity within each manifold. We let B_2 denote the energy eigenbasis that diagonalizes ρ_1 and divides the state space into degenerate angular-momentum manifolds. Appendix A shows that ρ_1 is invariant under time reversal, and that as a consequence, the manifolds of B_2 are related to the manifolds of B_1 through multidimensional rotations R_F.

These conclusions can be generalized to NH-PHIP. During the polarization period, the analyte molecule is a ligand that dissociates from a metal complex. Since the dissociation removes spins from the network of scalar couplings and causes the loss of correlations between the spins of the molecule and the spins that remain in the complex,[5] the evolution of spin order cannot simply be described as a process of averaging coherences. However, the structure of the scalar order at the end of the polarization period is the same for hydrogenative PHIP and NH-PHIP. During the polarization period, we can consider the spins of the entire sample to be governed by a scalar-coupling Hamiltonian whose terms are modulated by the binding and dissociation processes. Evolution under this spherically symmetric spin Hamiltonian converts the singlet spin order of parahydrogen molecules into scalar spin order in the sample, which to a good approximation is limited to individual molecules. The density matrix ρ_1 that represents the resulting ensemble of analyte molecules is therefore a scalar operator. Under the assumption that the oscillating coherences in the density matrix do not survive averaging over the distribution of times that follow the final dissociation of the molecule from the complex, the matrix elements of ρ_1 between states of different energy are zero, which implies that it commutes with H_J. The arguments of the previous paragraph show that ρ_1 can be diagonalized by an energy eigenbasis B_2 that divides the state space into manifolds (F, E), with ρ_1 proportional to the identity within each manifold. Basis B_1 is formed by addition of angular momenta, with the heteronucleus added last. This basis divides the state space into manifolds (F, I). For NH-PHIP as well as well as for hydrogenative PHIP, ρ_1 is invariant under time reversal, as shown in Appendix A, and the mixing of manifolds (F, I) to form manifolds (F, E) can thus be described by means of rotation matrices R_F.

[1] C. R. Bowers, "Sensitivity enhancement utilizing parahydrogen," in *Encyclopedia of Magnetic Resonance* (Wiley, 2007).
[2] C. Bowers and D. Weitekamp, J. Am. Chem. Soc. **109**, 5541 (1987); Phys. Rev. Lett. **57**, 2645 (1986).
[3] M. Pravica and D. Weitekamp, Chem. Phys. Lett. **145**, 255 (1988).
[4] R. W. Adams, J. A. Aguilar, K. D. Atkinson, M. J. Cowley, P. I. P. Elliott, S. B. Duckett, G. G. R. Green, I. G. Khazal, J. López-Serrano, and D. C. Williamson, Science **323**, 1708 (2009).
[5] R. W. Adams, S. B. Duckett, R. A. Green, D. C. Williamson, and G. G. R. Green, J. Chem. Phys. **131**, 194505 (2009).
[6] N. M. Zacharias, H. R. Chan, N. Sailasuta, B. D. Ross, and P. Bhattacharya, J. Am. Chem. Soc. **134**, 934 (2012); E. Y. Chekmenev, J. Hövener, V. A. Norton, K. Harris, L. S. Batchelder, P. Bhattacharya, B. D. Ross, and D. P. Weitekamp, *ibid.* **130**, 4212 (2008); K. Golman, O. Axelsson, H. Jóhannesson, S. Månsson, C. Olofsson, and J. Petersson, Magn. Reson. Med. **46**, 1 (2001).
[7] S. B. Duckett and N. J. Wood, Coord. Chem. Rev. **252**, 2278 (2008).
[8] M. B. Franzoni, L. Buljubasich, H. W. Spiess, and K. Münnemann, J. Am. Chem. Soc. **134**, 10393 (2012).
[9] E. Vinogradov and A. K. Grant, J. Magn. Reson. **194**, 46 (2008).
[10] L. Bouchard, S. Burt, M. Anwar, K. Kovtunov, I. Koptyug, and A. Pines, Science **319**, 442 (2008).
[11] M. S. Anwar, J. A. Jones, D. Blazina, S. B. Duckett, and H. A. Carteret, Phys. Rev. A **70**, 032324 (2004).
[12] T. Theis, P. Ganssle, G. Kervern, S. Knappe, J. Kitching, M. P. Ledbetter, D. Budker, and A. Pines, Nat. Phys. **7**, 571 (2011).
[13] T. Theis, M. P. Ledbetter, G. Kervern, J. W. Blanchard, P. J. Ganssle, M. C. Butler, H. D. Shin, D. Budker, and A. Pines, J. Am. Chem. Soc. **134**, 3987 (2012).
[14] J. W. Blanchard, M. P. Ledbetter, T. Theis, M. C. Butler, D. Budker, and A. Pines, J. Am. Chem. Soc. **135**, 3607 (2013).
[15] M. C. Butler, M. P. Ledbetter, T. Theis, J. W. Blanchard, D. Budker, and A. Pines, J. Chem. Phys. **138**, 184202 (2013).
[16] M. Ledbetter, C. Crawford, A. Pines, D. Wemmer, S. Knappe, J. Kitching, and D. Budker, J. Magn. Reson. **199**, 25 (2009).
[17] D. B. Zax, A. Bielecki, K. W. Zilm, A. Pines, and D. P. Weitekamp, J. Chem. Phys. **83**, 4877 (1985); D. Zax, A. Bielecki, K. Zilm, and A. Pines, Chem. Phys. Lett. **106**, 550 (1984); D. P. Weitekamp, A. Bielecki, D. Zax, K. Zilm, and A. Pines, Phys. Rev. Lett. **50**, 1807 (1983).
[18] D. Yu, N. Garcia, and S. Xu, Concepts Magn. Reson. **34A**, 124 (2009).
[19] D. Budker and M. Romalis, Nat. Phys. **3**, 227 (2007).
[20] I. M. Savukov and M. V. Romalis, Phys. Rev. Lett. **94**, 123001 (2005).
[21] V. Shah, S. Knappe, P. D. D. Schwindt, and J. Kitching, Nat. Photonics **1**, 649 (2007).
[22] M. Goldman and H. Jóhannesson, C. R. Phys. **6**, 575 (2005); H. Jóhannesson, O. Axelsson, and M. Karlsson, *ibid.* **5**, 315 (2004); M. Haake, J. Natterer, and J. Bargon, J. Am. Chem. Soc. **118**, 8688 (1996).
[23] S. Aime, R. Gobetto, F. Reineri, and D. Canet, J. Magn. Reson. **178**, 184 (2006).

[24]J. Natterer, O. Schedletzky, J. Barkemeyer, J. Bargon, and S. Glaser, J. Magn. Reson. **133**, 92 (1998).
[25]C. Cohen-Tannoudji, B. Diu, and F. Laloë, *Quantum Mechanics* (Wiley, New York, 1977), pp. 1072–1085.
[26]M. Auzinsh, D. Budker, and S. Rochester, *Optically Polarized Atoms: Understanding Light-Atom Interactions* (Oxford, New York, 2010).
[27]C. Cohen-Tannoudji, B. Diu, and F. Laloë, *Quantum Mechanics* (Wiley, New York, 1977), pp. 1054–1055.
[28]R. H. Dicke, Phys. Rev. **93**, 99 (1954).
[29]R. R. Ernst, G. Bodenhausen, and A. Wokaun, *Principles of Nuclear Magnetic Resonance in One and Two Dimensions* (Clarendon Press, Oxford, 1987), pp. 34–37.
[30]J. Natterer and J. Bargon, Prog. Nucl. Magn. Reson. Spectrosc. **31**, 293 (1997).
[31]See supplementary material in T. Theis, M. P. Ledbetter, G. Kervern, J. W. Blanchard, P. J. Ganssle, M. C. Butler, H. D. Shin, D. Budker, and A. Pines, J. Am. Chem. Soc. **134**, 3987 (2012).
[32]C. J. Lee, D. Suter, and A. Pines, J. Magn. Reson. **75**, 110 (1987).
[33]A. Messiah, *Quantum Mechanics* (Wiley, New York, 1959), Chap. XV.